

A
Project report
on
Thermo-hydrodynamics of single phase flow in
microchannel with obstacles

By
Bright Rose

ROLL NO: 212ME3317

Under the guidance of
Dr. MANOJ K. MOHARANA



Department of Mechanical Engineering
National Institute of Technology Rourkela
Rourkela-769008
June-2014



**NATIONAL INSTITUTE OF TECHNOLOGY
ROURKELA**

CERTIFICATE

This is to certify that the thesis entitled, “**Thermo-hydrodynamics of single phase flow in microchannel with obstacles**” submitted by **Mr. Bright Rose (212ME3317)** in partial fulfillment of the requirements for the award of Master of Technology Degree in **Mechanical Engineering** with specialization in **Thermal Engineering** at the National Institute of Technology, Rourkela (Deemed University) is an authentic work carried out by him under my supervision and guidance.

To the best of my knowledge, the matter embodied in the thesis has not been submitted to any other University/ Institute for the award of any degree or diploma.

Date:

Dr. Manoj Kumar Moharana
Department of Mechanical Engineering
National Institute of Technology Rourkela
Rourkela– 769008

SELF DECLARATION

I, Mr Bright Rose, Roll No. 212ME3317, student of M. Tech (2012-14), Thermal Engineering at Department of Mechanical Engineering, National Institute of Technology Rourkela do hereby declare that I have not adopted any kind of unfair means and carried out the research work reported in this thesis work ethically to the best of my knowledge. If adoption of any kind of unfair means is found in this thesis work at a later stage, then appropriate action can be taken against me including withdrawal of this thesis work.

NIT Rourkela

02 June 2014

Bright Rose...
Bright Rose

ACKNOWLEDGEMENT

I am extremely fortunate to be involved in an exciting and challenging research project like “**Thermo-hydrodynamics of single phase flow in microchannel with obstacles**”. It has enriched my life, giving me an opportunity to work in a new environment of ANSYS (FLUENT). This project increased my thinking and understanding capability as I started the project from scratch.

I would like to thank and express my gratitude towards my supervisor **Dr. Manoj Kumar Moharana** for his extensive support throughout this project work. I am greatly indebted to him for giving me the opportunity to work with him and for his belief in me during the hard time in the course of this work. His valuable suggestions and constant encouragement helped me to complete the project work successfully. Working under him has indeed been a great experience and inspiration for me.

Date:

Place:

Bright Rose

ABSTRACT

A numerical simulation has been carried out to understand the thermo-hydrodynamics of single phase flow with obstacle in microchannel. In this study, two different shapes of obstacle are analyzed with five different substrate materials to study the effect of thermal conductivity on the heat transfer. Uniform heating source is present at bottom wall of microchannel and remaining walls are kept adiabatic. The flow rate is maintained such that flow will be laminar theoretically. But under influence of obstacle, fluid is likely to get disturbed as it flows past the obstacle. So, both laminar and turbulent model was used in this analysis. The other factor is considered is the position of obstacle in the flow. The positions of obstacle affect the mixing of layer of fluid. Analysis reveals that position of obstacle in the flow field directly affect the heat transfer. Disturbance created at the initial stage carried to long distance which enhance heat transfer coefficient. It is found that the temperature difference between wall and fluid increase along the axial direction of flow except near the obstacle. In analysis, it is found that shape of obstacle directly affect the Nusselt number, for half obstacle variation of Nusselt number increase vibrantly as compared to full obstacle. In case of laminar model, it does not take account of eddies formation near the flow. Nor it accounts the surface roughness. While in turbulent model, eddies formation near the surface can be seen which in turn increase Nusselt number, when simulating both full and half obstacle using both laminar and turbulent model, it is found that higher Nusselt number is found in case of turbulent model, hence Nusselt number is reach to maximum in turbulent in comparison to laminar model.

Keywords: microchannel, heat transfer, obstacle, laminar and turbulent flow.

Nomenclature

C_{ps}	Specific heat capacity of solid density, J/kg K
C_{pw}	Specific heat capacity of fluid (water) J/kg K
D_h	Hydraulic diameter, mm
h	Coefficient of heat transfer, W/m K
k_f	Thermal conductivity of fluid, W/m ² K
k_s	Thermal conductivity of solid, W/m ² K
k_{sf}	Ratio of thermal conductivity of solid and fluid
L	Length of the Microchannel, mm
Nu	Local Nusselt number
\overline{Nu}	Average Nusselt number
Pr	Prandtl number
Q_w	Heat flux at wall (W/m ²)
Re	Reynolds number
T_f	Bulk mean temperature, K
T_w	Wall temperature, K
Z	Axial distance in Z direction, mm

Greek symbols

μ	Dynamic viscosity of fluid
τ	Shear stress
ρ_f	Density of fluid
ρ_s	Density of solid
α	Thermal diffusivity
ε	Turbulent dissipation rate

Subscript

f	Fluid
s	Solid
w	Wall

Content

Abstract

List of figures

List of tables

Nomenclature

1	Introduction	1-9
1.1	What are microchannels and their need?	1
1.2	Turbulent problem	3
1.3	Introduction to turbulence/ wall bounded turbulent flows	4
1.4	Reynolds Average Navier–Stokes based Model	4
1.5	Linear Eddy Viscosity Models	4
1.6	Linear eddy viscosity models	5
1.7	Two Equation Models	5
1.8	k- ϵ model	6
1.9	Turbulent Governing Equations	7
1.10	Turbulent Intensity	7
1.11	Turbulent Scale	8
1.12	Free Turbulent Shear Flow	8
1.13	Fully developed pipe flow	9
2	Literature review	10-15
3	Numerical simulation	16-21
3.1	Introduction	16
3.2	Detailed data	17-19
3.3	Grid independence test	20-21
4	Results and discussion	22-36
5	Conclusion	37
	References	38-40

List of Figures

Figure	Description	Page No.
1	Eddies formation at the rear face of obstacle	3
2	Instantaneous temperature at the bottom face	3
3	Three dimensional view of microchannel with obstacle	19
4	Front view and side view of the microchannel	19
5	Microchannel with flow direction	19
6	Nusselt number variation along the axial direction for three different size grids	21
7	Temperature profile of fluid and wall	21
8	Variation of heat transfer coefficient along the length of microchannel	23
9	Enlarge view of heat transfer coefficient	23
10	Effect of thermal conductivity on Nusselt number	24
11	Enlarge view of variation of Nusselt number due to thermal conductivity when obstacle is at 2 mm from inlet	24
12	Effect of thermal conductivity on Nusselt number	25
13	Enlarge view of variation of Nusselt number due to thermal conductivity when obstacle is 20 mm from inlet	25
14	Effect of thermal conductivity on Nusselt number using k- ϵ model	26
15	Enlarge view of variation of Nusselt number due to thermal conductivity	26
16	Variation of Nusselt number when position of obstacle is at 2 mm	27
17	Variation of Nusselt number when position of obstacle is at 20 mm	28
18	Variation of Nusselt number when full obstacle is placed in the flow field considering Laminar flow	28
19	Enlarge view of Nusselt number curve near the obstacle region	29
20	Variation of Nusselt number when full obstacle is placed in the flow field considering turbulent flow	29
21	Enlarge view of Nusselt number curve near obstacle region	30
22	Comparison of Nusselt number for full and half obstacle	30
23	Enlarge view of Nusselt Number for full and half obstacle	31
24	Variation of Nusselt number when half obstacle is placed in the flow field considering laminar flow	32

25	Enlarge view of Nusselt number curve near the obstacle region	32
26	Variation of Nusselt number when half obstacle is placed in the flow field considering turbulent flow	33
27	Enlarge view of Nusselt number curve near the obstacle region	33
28	Comparison of Nusselt number for full and half obstacle using turbulent model	34
29	Enlarge view of Nusselt Number for full and half obstacle using turbulent model	34
30	Variation of Nusselt Number for full obstacle using laminar/turbulent model	35
31	Enlarge view of Nusselt Number near the obstacle zone.	35
32	Variation of Nusselt Number for half obstacle using laminar/turbulent model	36
33	Enlarge view of Nusselt Number near the obstacle zone	36

List of tables

Table	Description	Page No.
1	Different material with their properties	17

Chapter 1

Introduction

1.1. What are microchannels and their need?

With advances in manufacturing methods, different innovative and unique devices ranging from very big to very small are being developed for different engineering applications. Recent developments in micromachining led to development of many microscale devices for engineering applications. Some typical applications of micromachining in the field of fluid flow and heat transfer can be found in [1]. One of them is microchannel which finds its wide applications. Microchannel can be described as channel of dimensions less than 1 mm and greater than one micron. Channels above one millimetre have same characteristics as conventional channels therefore the channels whose diameter are above 1 mm are consider as macrochannels. Microchannel characteristic diameter varies from 1 micron to 100 of microns. Microchannel provides advantage of high surface to volume ratio. As the volume decreases, surface area decrease but the scales of decrease of these two quantities are different. Volume decrease more than surface area and hence microchannel provide the high surface area to volume ratio. Due to high surface area to volume ratio of microchannel heat transfer coefficient enhances. Due to these properties, microchannel is widely used in electronic devices, micro heat exchangers etc. Microchannel is very helpful in biological field also. Microchannels are used to transfer biological material like DNA, Protein, cells and embryos. The industrial examples of microchannel are inkjet printing head, heat exchangers in computer cooling etc. to name a few.

Microchannels are different from macrochannel for two reasons: (i) microchannel takes account of molecular effects, no slip condition can be changed, and velocity at the wall surface can be taken as some finite value. Other property that is important is temperature. A temperature jump can be considered. (ii) The pressure drop across the channel is larger as compared to conventional channel.

The molecular structure of gas and liquid are different. Therefore they behave differently in same surrounding conditions. In case of micro-channel, a dimensional less number has to be introducing to differentiate the flow of gas and liquid in micro-channels. Knudson number is the parameter that decides the behaviour of micro-channel.

number is the parameter that divides the flow in continuum or outside continuum. Non-equilibrium condition begins to rise when the continuum fails. Hence in case of failure of continuum or Knudsen number between 0.1 and 0.001, modification needed in the slip boundary conditions. As the Knudsen number increases, assumption made in continuum are not valid. Study of non continuum flow requires different physical phenomena.

Due to difference in density of liquid and gas, spacing between the molecules is different. The densities of liquids are 1000 times greater than gases. Therefore the molecular spacing in liquids is about ten times greater than gases. For water, this spacing is 0.3 nm. Turkerman and Pease [2] has described that microchannel are capable of extracting large amount of heat and thus act as heat sink. Therefore they are valuable in electronics equipment's likes IC's, transistors etc. Heat extraction from any surface is function of specific heat capacity, surface area and temperature difference of walls and flowing fluid. For electronic equipments, temperature are restricted to certain limits, therefore more emphasis is done on surface area and temperature difference of walls and fluid. Due to higher surface area/volume as compared to conventional channel, microchannel provides high heat extraction.

Macro-channel and microchannel:

Microchannel is of order of 0.1 mm and macro-channel is conventional size of channel. For microchannel hydraulic diameter to solid wall thickness is of order one, while in case macro-channel hydraulic diameter to solid wall thickness is less than unity. In context to the flow in microchannel, a dimensionless number has to be calculated before carrying out any experiment, Knudsen number. Knudsen number is defined as molecular mean path to hydraulic diameter. For conventional channel, analysis and result are carried out based on continuum and thermodynamics equilibrium. Conservation equations are applicable if continuum assumptions are valid. As the channel size decrease Knudsen number increases, and at certain value continuum violates. Nearly Knudsen number around 0.1, continuum fails. Thermodynamics equilibrium fails leads to violation of no slip and no temperature jump at boundary conditions. Therefore Knudsen number should be lower than 0.001.

Extensive research is carried out from last two decades on fluid flow and heat extraction in microchannels. Still no particular standard formulae and equation is derived for microchannels, and still unsolved. Microchannel constitute complex nature of phenomena, there are various factor which still are not well understood like Reynolds number, channel size, surface roughness, heat dissipation etc.

Number of researches has shown that Navier-Stokes equations are not valid for microchannel. In order to use microchannel in micro devices, fluid flow need to be better understood. Some effect which has been neglected in macro-channel fluid flow need to be examined to study the microchannel fluid flow. Microchannel phenomena which need to be considered it two and three dimensional transport properties. In case of microchannel, characteristic diameter reduces and in same order hydro-dynamics boundary layer thickness. Second effect which can be considered is temperature variation in the fluid flow. It is assumed that fluid properties remain constant in the flow, but the in case of microchannel fluid properties can be change like density, viscosity. Sometimes thermal conductivity of fluid may also vary under the effect of temperature variation.



Figure 1: eddies formation at the rear face of obstacle



Figure 2: instantaneous temperature at the bottom face

1.2. Turbulent problem

The formation of turbulent flow develops from laminar flow when the Reynolds number increases above the critical value. This deviation happen when small disturbances to the flow cannot be damped by the viscous force present in the flow. When this disturbance increase and begin to grow by using energy from the original flow. This varied behaviour can be easily seen by watching the simple pipe flow with a obstacle in the pipe. When the flow is very small then the presence of obstacles does not affect the flow much, and flow is still can be laminar. When the Reynolds number increase to certain level when the presence of obstacle made effect on the floe and creating eddies in the flow, these eddies grow rapidly and disturbance is created along the flow, which leads to the condition of turbulence. Eddies formed grows by extracting energy from the original flow.

The manner in which the disturbance created and grow can be deduced from the equation. Equations are derived by dividing the motion in to mean and fluctuating component. Mean flow component is considered as laminar and fluctuating component is turbulent part. When the summation of turbulent part is taken, its result to zero as to conservation of energy concept holds. Separate equations for both the flow are formulated. Fluctuating components form some parameters which depend on the geometry of the channel. These equations of both mean and fluctuating component are substituted in the Navier-Stoke's equation. Averaging the fluctuating component leads to zero of the properties like velocity etc.

Turbulent model consist of Reynolds stress that makes it complex. Reynolds stress is said to be stress but it is very different from the viscous stress, the concept behind this different from fluid mechanics point of view. The Reynolds stress can be co- related to the other flow properties like velocity, momentum etc, which depends upon fluid properties. The reason behind this approximation is taking average over characteristic length and time which much smaller than the original flow. On the other hand, eddies formed is larger than molecular length causing the momentum transfer. Further details are available in [3].

1.3. Introduction to turbulence/ wall bounded turbulent flows

In the presence of walls or surfaces, disturbance in flow cannot be generated. The reason is that velocity or any rotation component of velocity come in direct contact brought to rest and hence satisfies the no-slip condition. The vorticity/eddies generated at the leading edge of surface/wall and then can be transported by diffusing and increase its magnification at next stage. Turbulence can be initiated at the wall only, and then at next stages. Once the fluctuating component of velocity has been generated, eddies go on to developing in the absence of surfaces. No slip condition comes from the concept that the fluid particles velocity at the surface is equal to the velocity of surface. If the surface is in rest, fluid particle is also at rest. This concept is used in all the conventional channel where concept of continuum is valid, if the continuum is invalid then the condition of slip and temperature jump may arise. The parameter which divides the continuum validity is Knudsen number.

1.4. Reynolds Average Navier-Stokes based Model

The principle aim of RANS turbulent models is to calculate the Reynolds stress.

Here are three models which calculate the Reynolds stresses.

1. Linear eddy viscosity models

2. Nonlinear eddy viscosity models
3. Reynolds stress model (RSM)

1.5. Linear Eddy Viscosity Models

LEV models are the turbulent models. These models describe the Reynolds stress which is deduced from the RANS, and converted in to linear relations to the average velocities of flow stream.

LEV models are divided in to the following models. LEVM division depends on the transport variable in the equation and the number of equations that help in calculating the eddy viscosity.

- (a) One equation models
- (b) Two equation models

1.6. Linear eddy viscosity models

LEV models are divided in two divisions:

- A. One equation models
- B. Two equation models

Two equation models are sub divided in to two parts

1. K- ϵ model
2. K- Ω model

These models itself divided in two sub-categories

1. K- ϵ models
 - i. Standard k- ϵ model
 - ii. Realisable k- ϵ model
 - iii. RNG k- ϵ model
 - iv. Near-wall treatment
2. K- Ω models
 - i. Wilcox's k- Ω model
 - ii. Modified Wilcox's k- Ω model
 - iii. SST model

1.7. Two Equation Models

The most widely used models of turbulent flow are k-epsilon model and the k-omega model. They are extensively used in industry and research analysis. These models are active in research field and two new equations are developing.

Two equation models consist of transport properties of turbulent flow. Two equations were developed to calculate the intensity of disturbance. These equations will heed of convection and diffusion effect.

Turbulent energy is one of the transport parameter. On the other hand, other transport parameter depends on type of model in use. Dissipation is used as second property, dissipation is of two types and hence equation also divides in two forms. Turbulent Dissipation & specific dissipation are the two forms of dissipation. Dissipation describes the scale in the flow whereas TKE describes the energy.

1.8. k- ϵ model

The k- ϵ model is one of the popular turbulent models that has been using widely in the analysis of disturbance/turbulence. Its performance decrease when large pressure drop occurs across the flow. It is based on the two model equation, it normally represent two extra equations other than conservation equation. These two equations are the transport properties of the flow. These equations help in evaluating the turbulence properties. These two equations are the symbolic of convection and the diffusion in the TKE.

The two new variables in the equation are turbulent kinetic energy and dissipation. These two variable are the transport variable in the equation. These two variables calculate the disturbance and energy in the flow field. k calculates the energy in the flow and epsilon calculates the scale in the flow.

The main aim of the k- ϵ model was to enhance the mixing length and to algebraically describe the disturbance scale in complex flows.

The k- ϵ model is work extremely good in small pressure variation. These models describe the free shear layer flows well. Near wall region or pipe flow, this model provides good results in low pressure variation. Level of accuracy is high for small pressure variation than the large pressure variation. This model will become worst in case of compressors.

The basic of turbulence modelling is to divide instantaneous velocity in to mean velocity and fluctuating velocity, and solving the mean velocities. The effect of fluctuating velocities is taken in account after deriving empirical relation from experiment. Navier-Stokes equation along with conservation of mass and energy forms a group of equations.

Decomposing velocities in mean and fluctuating velocities, number of unknown increases and equation remains the same. Conservation equation are alone not sufficient to solve the unknown therefore, empirical relation (derived from experiment) are included to solve the unknowns. The local turbulent viscosity is calculated from the solution of transport equations for the turbulent kinetic energy (k), and (ϵ) the rate of dissipation of turbulence energy. Further details are available in [4].

1.9. Turbulent Governing Equations

Turbulent Kinetic Energy (K)

$$\rho \frac{\partial k}{\partial t} + \rho \frac{\partial k u}{\partial x_i} = \rho \frac{\partial}{\partial x_j} \left[\left(v + \frac{v_t}{\sigma_1} \right) \frac{\partial k}{\partial x_j} \right] + G_1 + G_2 - \rho \epsilon - Z_M + S_1 \quad (1.1)$$

Turbulent Dissipation (ϵ)

$$\rho \frac{\partial \epsilon}{\partial t} + \rho \frac{\partial \epsilon u}{\partial x_i} = \rho \frac{\partial}{\partial x_j} \left[\left(v + \frac{v_t}{\sigma_2} \right) \frac{\partial \epsilon}{\partial x_j} \right] + c_{1e} \frac{\epsilon}{k} (G_1 + C_{3e} G_2) - c_{2e} \rho \frac{\epsilon^2}{k} + S_2 \quad (1.2)$$

$$c_{1e} = 1.44 \quad c_{2e} = 1.92 \quad c_{3e} = -0.33 \quad c_{\mu} = 0.09 \quad \sigma_1 = 1.0 \quad \sigma_2 = 1.3$$

$$v_t = C_{\mu} \frac{k}{\epsilon^2}$$

$$G_1 = \rho v_t S$$

1.10. Turbulent Intensity

The turbulence intensity is defined as the ratio of the RMS value of velocity to the mean free velocity in the flow region. Generally intensity is denoted by I.

RMS value of the fluctuating component of the velocity in all three directions and mean free velocity is the velocity with any loss of friction. Or in other word can be said that it the velocity at inlet of pipe flow.

Before setting boundary condition in simulation of problem, it is important to calculate the intensity at the inlet. It will be the better option to measure or estimate from previous experimental data.

- (a) Low turbulence intensity: low velocity flow with simple structure geometry. The low intensity case limit when the value of intensity is below 2%. Simple pipe flow, flow over the plate, sub-marines etc are the examples.

- (b) Moderate turbulent intensity: medium speed flow with low complex geometry. Intensity varies from 2% to 4%. Flows in rotating components are the examples of moderate intensity.
- (c) Large turbulent intensity: it occurs in high speed flow. The other possibilities of large intensity are the complex shape of the structure. Like flow in compressors, flow over high speed car, storm-thunders etc.

$$T.I = \frac{4}{25} Re^{-0.125} \quad (1.3)$$

$$V^* = \left(\frac{u^{*2} + v^{*2} + w^{*2}}{3} \right)^{(0.5)} \quad (1.4)$$

$$V = \left(u^2 + v^2 + w^2 \right)^{(0.5)} \quad (1.5)$$

$$I = \frac{V^*}{V} \quad (1.6)$$

1.11. Turbulent Scale

The turbulent scale is the entity that describes the size of the eddy. It also calculates the energy in the following eddy in disturbed flow. The turbulent scale calculates the disturbance properties at the inlet. It is the entity which co-relates the size of eddy. Turbulent scale cannot be larger than the physical dimension of the structure. In other words, eddies cannot be larger than the structure.

$$\text{Turbulent scale} = C_{\mu} \frac{k^{1.5}}{\varepsilon} \quad (1.7)$$

1.12. Free Turbulent Shear Flow

Free shear flow is the flow with average velocity variation developed in the absence of boundaries. Free turbulent free flows are found in free convection environment. Some of the examples are air coming out of nose/mouth during respiration rings during smoking fumes during the volcano eruption etc. These all examples of free turbulent shear flow can be found easily in nature. some example from engineering point of view are, wakes formed while car is moving, wakes formed at the rear side of car, exhausts from the engines etc. Many mixing & exhaustion processes forms free turbulent flow shear.

Free shear flow are generally turbulent type. If they are produced in the laminar form they have tendency to convert in the turbulent very rapidly. The reason behind this is the vorticity developed very fast when the surface is not present.

The important behaviour of free shear flows that it form turbulence and remain in turbulent, they can be upgrade by the presence of density variation across the flow. It also takes account of gravitational forces. The proof of change of behaviour can be seen neglecting the viscosity in the vorticity equations.

1.13. Fully developed pipe flow

For fully developed pipe intensity can be calculated by the following formula

$$\text{Turbulent Intensity} = 0.16\text{Re}^{-0.125} \quad (1.8)$$

Literature Review

Microchannel study is not new concept, while a well developed concept. A review on microchannel with laminar as well as turbulent model is studied. Some are experimental work while other are simulated on CFD software.

Tullius et al. [5] have modelled finned mini-channel, to maximize heat transfer through convection effect. They modelled six different shapes- circle, triangle, square, ellipse, diamond and hexagon with staggered arrangement. Constant heat flux is provided on bottom surface of channel. They found triangular shape provide high heat transfer and enhance Nusselt number. Increase in fin height, increase Nusselt number. Decrease in fin width and spacing Nusselt number increases.

Peles [6] had conducted an experiment with pillar in microchannel with air as fluid flowing in it. Data were collected for Reynolds number between 100 and 5600. He has found that heat transfer coefficient with pillar in microchannel is twice the microchannel without pillar. And among three geometries, triangular give highest Nusselt number.

Peles et al. [7] calculated heat transfer and pressure drop phenomena in pin fin microchannel. They derived a relation for thermal resistance, and it has been found that low thermal resistance are achieved using pin fin heat sink.

Liu et al. [8], they conducted an experiment to predict heat transfer efficiency of high pin fin in microchannel, the experiment conducted shows that pressure drop and overall Nusselt number increase with fin Reynolds number. And propose two new correlations for Nusselt number and pressure drop.

Peles et al. [9] conducted an experiment to study single phase stagnation point jet impingement. Experiment conducted compare two case, (a) smooth microchannel, (b) micro pin fin structured microchannel. Micro pin-fin channel show mixing enhancement and increases Nusselt number.

Khan et al. [10] did an analytical model for determining heat extraction. They compare two cases (a) inline (b) staggered pin fin heat sinks, which are used in electronic applications. The effects of thermal conductivity are examined on thermal performance. The model show good agreement with experimental and numerical data for high Reynolds number. Mathematical equations formed for coefficient of friction and heat extraction for inline and staggered arrangements.

Roth et al. [11] also performed an analysis on inline and staggered fin array. Clearance to diameter ratio is considered as main parameter, and laminar regime is taken from Re 9 to 246. New heat transfer correlations are developed with a new parameter which considers the strong influence of the clearance to diameter ratio on overall heat transfer.

Qu and Ho [12] studied thermal and hydrodynamics characteristics of single phase flow. They express new relation that removes the over-prediction of previous six expressions for Nusselt number. The expression formed for average Nusselt number fairly the local Nusselt number data.

Ho and Qu [13] proposed a new relation predicting parameter for pressure drop across staggered micro pin fin array. This pat concerning water single phase pressure drop and heat transfer. Two cases are examined (a) adiabatic, (b) diabatic. These two are the boundary conditions.

Dutta et al [14] performed an experiment. A square cylinder is placed in the flow with different orientations and depicted the results. Difference in the formation of eddies with the change of orientations of square cylinder. Along with the orientation of cylinder, aspect ratio is also varied and its effect is also plotted.

Mittal [15] did computational study on three dimensional low aspect ratio flow through circular cylinder, and had taken three different Reynolds number to study the vortex shedding. They confirmed that end condition is major role in vortex shedding for finite cylinder. They had taken one of the end-walls as a no-slip wall while the other walls as slip wall.

Seyf and Layeghi [16] did a numerical analysis on forced convection heat transfer is studied on elliptical pin fin along with metal foam. Model is built in three dimensional models. The pin fin heat sink model consists of six elliptical rows. Author has used Dary-Brinkman-Forchheimer and Navier-Stokes equation for the analysis. The heat transfer coefficient/Nusselt number increase with the use of metal foam inserts. On the other hand average heat transfer coefficient increase with the decrease in Reynolds number.

Jasperson et al. [17] did an analysis on microchannel and macro-channel, performance of each is calculated and plotted, it is found that microchannel is far good in ejecting heat from the small area, and can act as excellent heat sink. Microchannel with pin fin has potential of extracting high amount of heat and as an alternate to replace conventional sink for small heat surface. An array of pin fin used for analysis. Thermal performance, hydraulic performance and cost of manufacturing as metrics are also compared.

Qu and Mudawar [18] done three dimensional study of rectangular microchannel fluid flow and analyzed numerical solution using water is cooling fluid. Numerical coding was done based on finite difference method. SIMPLE algorithm is used to solve conservation equations. The analysis is thoroughly studied and compared analytical solution as well as experimental solution. In analysis, it is found that temperature increase in the direction of flow in solid and fluid era can be considered as linear. The highest temperature occurs at the heated base surface near outlet. Heat flux and Nusselt number have higher value at inlet than anywhere else.

Qu and Mudawar [19] analyzed to check the effect of pressure drop and heat transfer characteristics microchannel heat sink, the study is carried out numerically as well as experimentally. Heat sink/microchannel is constructed by oxygen free copper. Heat sink has array of microchannel. De-ionized water is used in as working fluid instead of normal water. A steady slope change is found in pressure drop across the inlet outlet with Reynolds number, change of flow from laminar to turbulent is found during analysis. Analysis conform good agreement of pressure drop and sink temperature of experimental data with numerical data, hence it can be concluded that Navier-Stokes and energy equation are varied.

Ho et al. [20] did experimental work to study the pressure drop and heat transfer characteristics of fin microchannel. Cooling fluid is de-ionised water in single phase. Variations of Reynolds number were considered. Average friction factor were calculated for pressure drop, and local Nusselt number/heat transfer coefficient. Experiment end up with some results, they concluded that friction factor calculated experimentally agree well with Moores and Joshi friction factor co-relations. Higher Local heat transfer coefficient found near heat sink at inlet and degrades along the length.

Zhou et al. [21] studied convective heat transfer and friction factor of silver nano-fluid. A model of microchannel is constructed with pin fin and act as heat sink experimentally. The use of surfactant increase fluid viscosity which in turn the pressure drops across the channel. Experiment shows that nano-particles improve heat transfer.

Guo and Li [22] modelled a microchannel and analysed the size effect on flow and heat extraction/ degradation. Fluid flowing inside microchaanel is gas, and hence they introduce the concept of continuum. Since microchannel has large surface area to volume, surface effects are of greater importance. Knudsen number is calculated. Kn should be of order of 0.001 to continue analysis in continuum otherwise it will lead to statistical approach. As surface to volume factor increase surface friction induce compressibility and that leads to velocity profile flatter in the channel and enhance friction factor and Nusselt number.

Lee et al. [23] investigated heat transfer experimentally; and also modelled a rectangular microchannel. The experiment was done to develop a relation taking account of macro-channel. Fluid flowing inside the channel is de-ionised water and a great variation of Reynolds number has taken in account. A continuum approach has been introduced to check the safeguard the microchannel from being out of statistical approach. On the other hand, numerical simulations were carried out based on Navier-Stokes equation. And both the result shows good agreement with each other.

Hetsroni et al. [24] studied on microchannel using gas and liquid as cooling fluids and using low Knudsen number and Mach number for continuum. A study on different pin fin structure is concentrated for analysis of pressure drop. Variation of Reynolds number is accounted to understand the transformation of laminar to turbulent flow. And checked the agreement between conventional methods with experimental result and check the other unexpected effect.

Morini [25] studied viscous heating in during the flow in microchannel. He demonstrated the effect of cross section on viscous heating. And describe the role of Reynolds number on flow heating. He formulated formula for minimum Reynolds number at which viscous dissipation can be overlooked. Formula is based on hydraulic diameter and geometry. He also matched the experimental result with conventional theory of Navier-Stokes equation. Friction factor is also considered as important parameter for pressure drop across the sections.

Hetsroni et al. [26] did experimental and numerical study for microchannel heat transfer. Previous part considers pressure drop and formation of turbulent from laminar flow. Four different shape pin fin were analysed and the geometric effect, axial conduction effect and energy dissipation are consider in examination. They examined the experimental data received from number of researchers and compared with conventional theory.

Lee and Garimella [27] did 3-D numerical simulations to understand the effect of convective heat transfer in entrance zone of laminar flow in rectangular microchannel. Two boundary conditions were considering (a) constant wall temperature (b) constant heat flux. Variation in aspect ratio is also considered. Both Nusselt number and average Nusselt number is calculated and plotted for constant temperature and constant heat flux. Formulas were designed for microchannel which shows good consent with other experimental results.

Moharana and Khandekar [28] performed a numerical study on rectangular pipe flow microchannel, to optimise the Nusselt number. They explained the effect of axial wall conduction and heat transfer with constant heat flux at bottom face of rectangular channel.

They also explained effect of thermal conductivity on heat transfer. They also depicted the dependency of substrate thickness to channel thickness.

Moharana et al. [29] performed numerical simulation and experiment for thermo-hydrodynamic performance of single phase flow. An array of rectangular microchannel was designed for experimental work and similar for numerical simulation. Microchannel array was fabricated on copper substrate. Reynolds number varies from 150 to 2500 and prandtl number from 3 to 4. Inlet pressure is kept at 1.1 bar. Transformation of laminar to turbulent flow is found at the Reynolds number 1100 for channel roughness 3.3 micro-meter. A 3 D model were designed to correspond to experimental geometry. In boundary condition lower channel wall is given constant heat flux. Based on the combined study they concluded that conjugate effects play vital role in mini/microchannel system and negligence of axial wall conduction leads to misleading conclusions.

Moharana and Khandekar [30] studied the axial conduction in microtubes. 2-D numerical simulation was carried out. Constant heat flux and constant temperature both condition were analysed at outer wall of microtube. The flow is taken as laminar. The cross sectional faces are considered as adiabatic. Different material of substrate was used and ratio of thermal conductivity of solid to liquid is the main parameter. Ratio of tube thickness varies from 1 to 16. Result clearly indicates k_{sf} plays important role in the conjugate heat transfer.

Moharana and Khandekar [31] studied conjugate heat transfer in three dimensional numerical simulations. The flow is considered as laminar in rectangular microchannel to evaluate the effect of aspect ratio on axial conduction in the substrate. A reference fixed size rectangular channel of dimensions 0.6 mm×0.4 mm×60 mm was used and variation in aspect ratio were done. Variation of aspect ratio follows the width to height from 0.45 to 4.0. the flow rate is low and Reynolds number is taken as 100. Simulation concluded with the result that maximum value of Nusselt number exists at the optimum value of thermal conductivity of solid to liquid.

Kumar and Moharana [32] carried out study on axial conduction in partially heated microtube. A 2D model was designed and numerical simulations were carried out to understand the effect of axial wall conduction. The flow is considered as laminar. Total length of microtube is taken as 60 mm. 6 mm length from inlet and outlet is kept insulated. The constant wall temperature condition was imposed on the microtube outer surface.

Tiwari et al. [33] carried out study on influence of axial conduction in partially heated microtube. In this study a numerical simulation were carried. The flow was considered as laminar and constant heat flux condition was imposed on the outer wall surface. Comparisons

were made with fully heated microtube. Total length of microtube is taken as 60 mm and 6 mm from both inlet and outlet end are insulated. Cross sectional face of microtubes are insulated. Variation in three parameter considered are Reynolds number, ratio of thermal conductivity of solid to liquid and ratio of wall thickness to inner radius. They found that wall thickness and conductivity play critical role in axial back conduction.

Numerical Simulation

3.1. Introduction

A study has been done on the thermo-hydrodynamics of single phase with obstacles/ribs. In this study, an obstacle is placed inside the rectangular channel and the effect of presence of obstacle is studied. Presence of obstacle on heat transfer coefficient and Nusselt number has been calculated. Simultaneously, the position of obstacle is also studied. In the numerical simulation, three position of obstacle is studied. The length of the rectangular channel is taken for simulation is 30 mm. And Reynolds number at which fluid flowing inside the channel is taken as 100. Corresponding to Reynolds number developing length was calculated. And the positions of obstacle are placed in the developed flow and hence the effect of flow developing zone is neglected. The two positions of obstacles are 2 mm, 20 mm. And third cases were also studied in which two obstacles are place inside the channel across the flow. The positions of the obstacles are 2 mm and 20 mm. In third case also heat transfer and Nusselt number were calculated.

To understand the variation of heat transfer and Nusselt number due to obstacles, two different obstacles are designed. Some researchers named these obstacles as rib in their researchers. Two ribs were designed, one half rib and second is full obstacles. Half rib is place at the centre of channel while a full obstacle is designed on the bottom face from other two adjacent walls. In both the cases, laminar and turbulent model were improvised.

In the previous researches, researchers consider flow is laminar when the Reynolds number is small even after placing obstacles/cylinder of different shape was placed in the flow field. In this study, both laminar as well as turbulent model is used. In the laminar model, it was considered that surface of walls are smooth and the streamline are parallel with each other. Friction factor were neglected. While in case of turbulent models, friction factor is not neglected, they are importantly considered as the shape/geometry of the channel. Turbulent models take account of all the other factors which were neglected in the laminar model. Numerical simulation is repeated for different materials to take account of thermal conductivity. A table is drawn that contain the important properties value of materials. The variation of Nusselt number and heat transfer coefficient has been calculated for all the case.

There are sixty cases that have been studied for both laminar and turbulent flow, full rib and half rib. Variation of each case has been plotted on the graph on the following pages.

A three dimensional model were prepared to study flow in rectangular microchannel pipe with obstacle/rib. Both laminar model and turbulent model were used to defect the effect of obstacle on flow. The formation of eddy can be detected by turbulent model. In this work, fluid flowing inside the channel is in single phase throughout the length of channel. Condition is taken as steady state for both laminar and turbulent model. Compressibility of fluid is neglected as fluid flowing is water. Constant heat flux is condition is used in all simulation, bottom wall of channel is given all heat and other walls are kept insulated. No lose of energy. Fluid flows through the channel at Reynolds number 100. Three different models were designed to check the variation of Nusselt number along length with obstacles. Positions of obstacles are different in these designed models. These three models are simulated in both laminar model and turbulent model to check Nusselt number variations. Variation of Nusselt number with different position of obstacles and flowing model is calculated. Graph of each are drawn to understand the eddy effect and vortex effect. Effect of material conductivity is also taken in account and different material is used in simulation and their effect is also depicted on graphs.

Table 1: List of materials with their properties

Material	Thermal conductivity	Density (ρ)	Specific heat capacity (C_p)	Thermal conductivity of water (K_w)	Relative thermal conductivity (K_{sf})
Bismuth	7.86	9780	122	0.6	13.1
Constantan	23	8920	384	0.6	38.33
Bronze	54	8780	355	0.6	90
Aluminium	202.4	2719	871	0.6	337.33
Silver	429	10500	235	0.6	715

3.2. The governing differential equations:

Continuity Equation

$$\frac{\partial \rho}{\partial t} + \nabla (\rho \mathbf{V}) = 0 \quad (3.1)$$

Momentum Equation's

$$\rho \left(\frac{\partial u}{\partial t} + \frac{\partial u}{\partial x} + \frac{\partial u}{\partial y} + \frac{\partial u}{\partial z} \right) = -\frac{\partial P}{\partial x} + \mu \left(\frac{\partial^2 u}{\partial x^2} + \frac{\partial^2 u}{\partial y^2} + \frac{\partial^2 u}{\partial z^2} \right) + F_x \quad (3.2)$$

$$\rho \left(\frac{\partial v}{\partial t} + \frac{\partial v}{\partial x} + \frac{\partial v}{\partial y} + \frac{\partial v}{\partial z} \right) = -\frac{\partial P}{\partial y} + \mu \left(\frac{\partial^2 v}{\partial x^2} + \frac{\partial^2 v}{\partial y^2} + \frac{\partial^2 v}{\partial z^2} \right) + F_y \quad (3.3)$$

$$\rho \left(\frac{\partial w}{\partial t} + \frac{\partial w}{\partial x} + \frac{\partial w}{\partial y} + \frac{\partial w}{\partial z} \right) = -\frac{\partial P}{\partial z} + \mu \left(\frac{\partial^2 w}{\partial x^2} + \frac{\partial^2 w}{\partial y^2} + \frac{\partial^2 w}{\partial z^2} \right) + F_z \quad (3.4)$$

Energy Equation

$$u \frac{\partial T}{\partial x} + v \frac{\partial T}{\partial y} = \alpha \left(\frac{\partial^2 T}{\partial x^2} + \frac{\partial^2 T}{\partial y^2} \right) + \frac{1}{\rho c} \phi \quad (3.5)$$

$$\phi = 2\mu \left[\left(\frac{\partial u}{\partial x} \right)^2 + \left(\frac{\partial v}{\partial y} \right)^2 + \frac{1}{2} \left(\frac{\partial v}{\partial x} + \frac{\partial u}{\partial y} \right)^2 - \frac{1}{3} \left(\frac{\partial u}{\partial x} + \frac{\partial v}{\partial y} \right)^2 \right]$$

Kinetic Turbulent Energy

$$\rho \frac{\partial k}{\partial t} + \rho \frac{\partial k u}{\partial x_i} = \rho \frac{\partial}{\partial x_j} \left[\left(\nu + \frac{\nu_t}{\sigma_1} \right) \frac{\partial k}{\partial x_j} \right] + G_1 + G_2 - \rho \varepsilon - Z_M + S_1 \quad (3.6)$$

Energy Dissipation

$$\rho \frac{\partial \varepsilon}{\partial t} + \rho \frac{\partial \varepsilon u}{\partial x_i} = \rho \frac{\partial}{\partial x_j} \left[\left(\nu + \frac{\nu_t}{\sigma_2} \right) \frac{\partial \varepsilon}{\partial x_j} \right] + c_{1e} \frac{\varepsilon}{k} (G_1 + C_{3e} G_2) - c_{2e} \rho \frac{\varepsilon^2}{k} + S_2 \quad (3.7)$$

3.3. Assumption in Modelling of Microchannel

The following assumptions are made to model the heat transfer in the rectangular channel:

- (1) Steady state,
- (2) Incompressible fluid,
- (3) Constant fluid properties,
- (4) Considered axial conduction and viscous dissipation, and
- (5) Negligible radiation and natural convective heat transfer from the microchannel heat sink.

3.4. Geometric View of Microchannel

- i. A rectangular microchannel of $0.8\text{mm} \times 0.6\text{mm} \times 30\text{mm}$.
- ii. For simplification of calculation and effect of mixing, half portion is considered.
- iii. Symmetry is drawn on half model.

A 3D view of microchannel as shown:

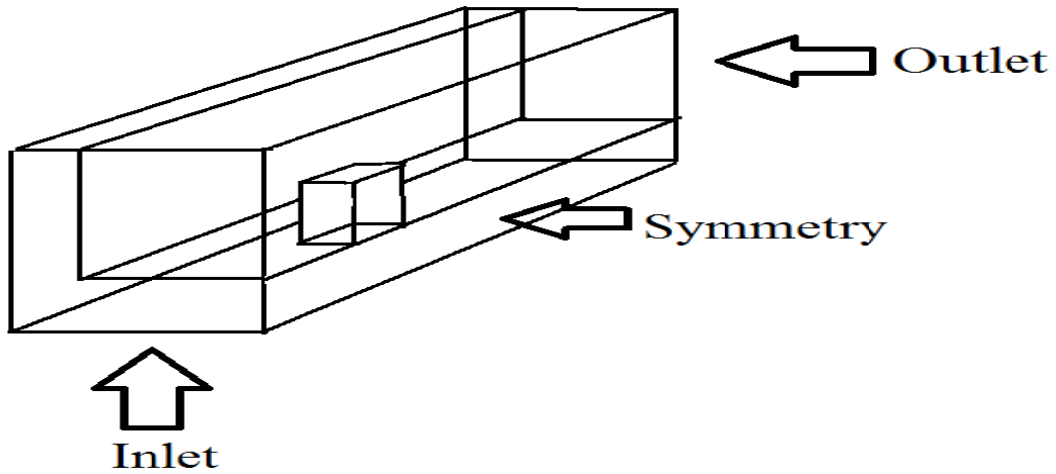


Figure 3: Three dimensional view of microchannel with obstacle

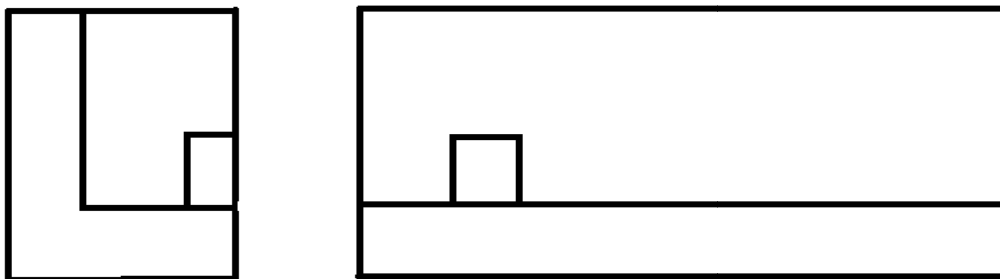


Figure 4: Front view and Side view of the Microchannel

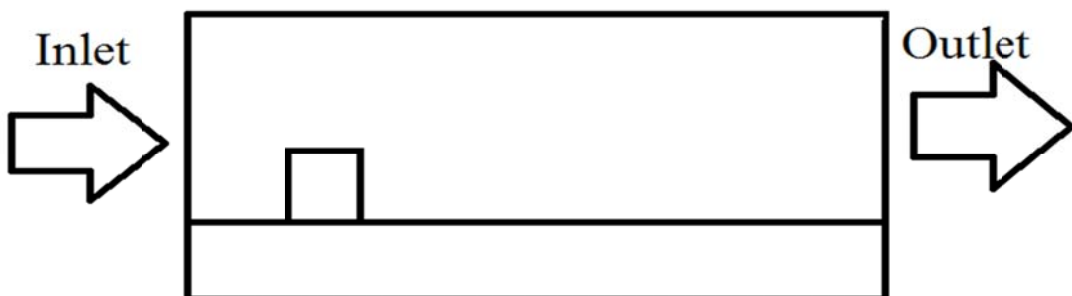


Figure 5: Microchannel with flow direction

3.5. Boundary conditions:

- i. heat flux on bottom wall (q'') W/m^2
- ii. Adiabatic Walls
 $Z = 0$ $Y = 0$ to $Y = 0.2\text{mm}$
 $Z = 30\text{mm}$ $Y = 0$ to $Y = 0.2\text{ mm}$
 $X = 0$, $Y = 0$ to $Y = 0.6\text{ mm}$, $Z = 0$ to $Z = 30\text{ mm}$
 $X = 0.2$, $Y = 0.2$ to $Y = 0.6\text{ mm}$, $Z = 0$ to $Z = 30\text{ mm}$
- iii. At Adiabatic wall $dq/dx = 0$, $dq/dy = 0$.
- iv. Temperature at adiabatic walls $dT/dx = 0$, $dT/dy = 0$.
- v. Velocity at solid surface is zero, $u = 0$, $v = 0$ (No Slip condition)
- vi. At $Z = 0$ (inlet) velocity of fluid $u = 0.2512\text{ m/s}$

These conservation and governing equations and their corresponding boundary conditions are solved by Ansys-Fluent[®]. The study of thermo-hydrodynamics of fluid flow with obstacles both laminar and turbulent models were used. Laminar model does not need any manipulation. In case of turbulent model, k- ϵ model is used. In k- ϵ model, two new transportation terms get introduced because of its properties. One is turbulent kinetic energy and second turbulent dissipation. K-epsilon model introduce two new governing equations, and six constants value are used. SIMPLE algorithm is used in Pressure Velocity coupling, discretization of pressure is taken as Standard, and for momentum and energy discretization technique is taken as Second Order Upwind. Under-Relaxation factors for density and energy is taken as 1 and pressure is 0.3 and momentum is 0.7. Convergence criteria for continuity and momentum are taken as 10^{-6} and for energy is 10^{-9} . The meshes that were generated are rectangular in shape and size is taken as 0.0133.

3.6. Grid independence test

A grid independence test has been performed to check which mesh size gives accurate result. And all further simulation was done on same mesh size. A simple pipe flow model is used for grid independence, and Nusselt number has been calculated for all the mesh size. Three meshes were tested for accuracy. Mesh size are $20 \times 30 \times 600$, $30 \times 45 \times 750$, $45 \times 60 \times 900$. The conditions for calculating Nusselt number are constant heat flux at bottom face of rectangular pipe and Reynolds number 100. It has been found through grid independence test that percentage error between $20 \times 30 \times 600$ and $30 \times 45 \times 750$ is 0.0012% whereas error between $30 \times 45 \times 700$ and $45 \times 60 \times 900$ were 0.0008%. Considering percentage error, mesh size $30 \times 45 \times 750$ has been selected for further simulation.

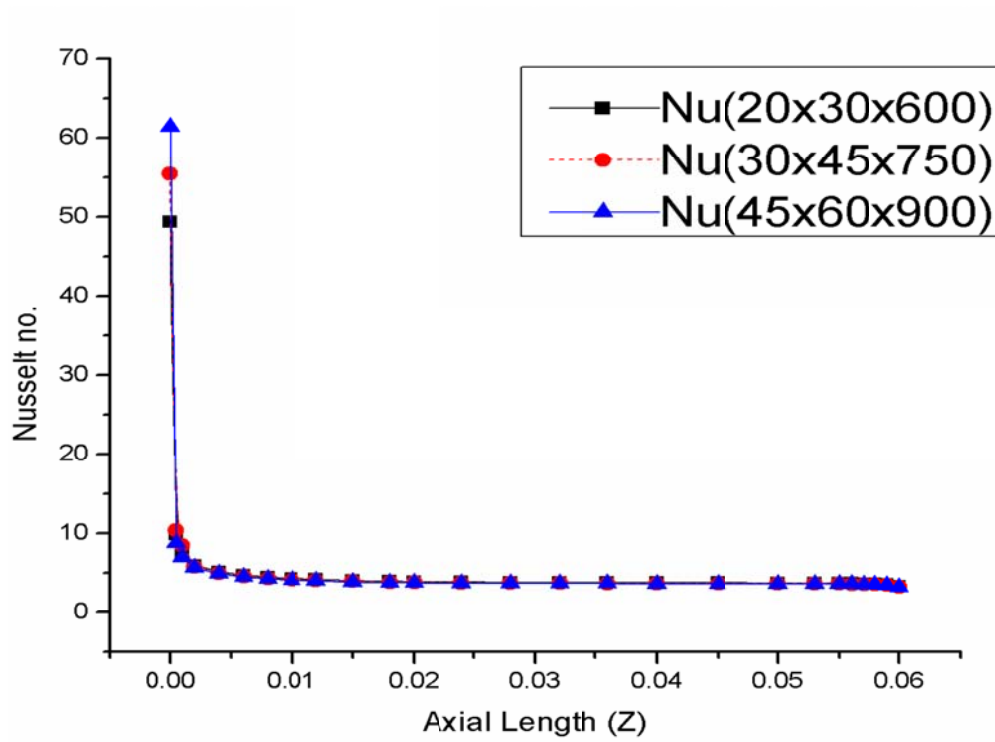


Figure 6: Nusselt number variation along the axial direction for three different size grids

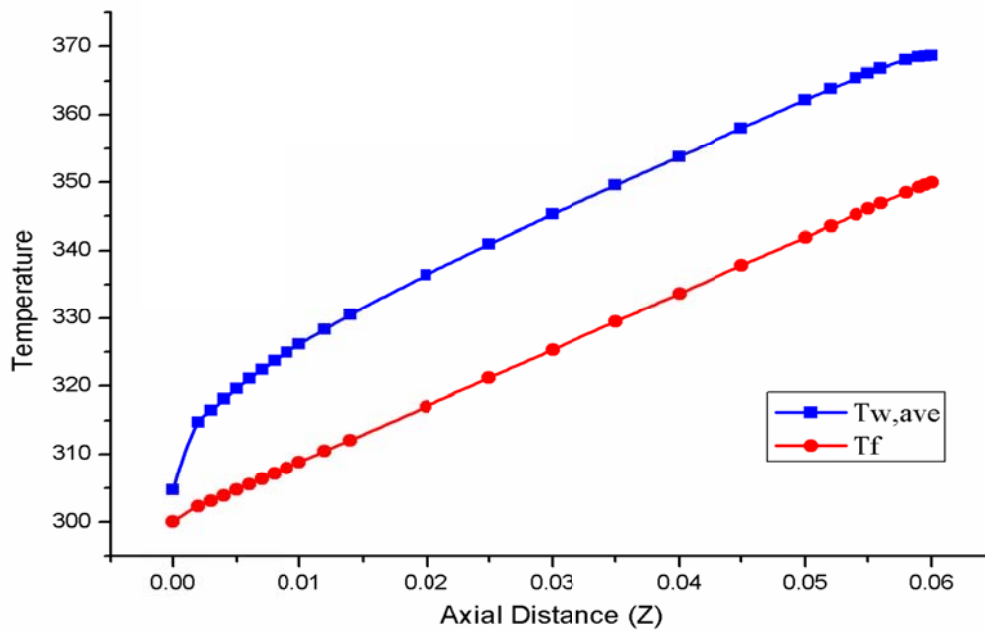


Figure 7: Temperature profile of fluid and wall

Results and Discussion

As the aim of numerical simulation, is to understand the thermo-hydrodynamics of single phase flow in microchannel with obstacle. There are two conditions at which the heat is transferred from the source (a) constant temperature (b) constant heat flux. Constant temperature is rarely found in the application. But constant heat flux is found application. Though theoretical analysis of circular pipe flow was done, and formula for heat transfer coefficient has been evaluated. Nusselt number for both the case in circular pipe has already been calculated, for heat temperature $Nu = 3.66$ while for constant heat flux $Nu = 4.36$. In this study a rectangular channel is designed and numerical simulation is performed. And corresponding Nusselt number is calculated. The study also includes the behaviour of flow in microchannel when an obstacle is present inside the channel.

The presence of obstacle effect the flow and due to diversion of streamline in the flow, mixing between the layers of fluid takes place, which enhance the heat dissipation of source. As the Reynolds number is low, it can be considered as the flow is laminar, but to study variation in heat transfer coefficient and Nusselt number in the presence of obstacle, turbulent model is also used. And both the models are compared. The graphs for both the models are plotted and deduce some results.

The position of obstacle is important parameter for mixing of fluid layers, which in turn affect the heat transfer rate. In the first case obstacle is placed at the end of hydrodynamic developing zone. In other words, obstacle is place at the beginning of fully developed zone. Since, Reynolds number for this study is constant and its value is taken as 100. Corresponding length of the developing zone is calculated by the formula.

$$X_h = 0.05 \times Re \times D_h$$

The calculated value for Re 100 for hydraulic diameter of 0.4 mm is 2 mm from the inlet. The dimension of obstacle is $0.4 \times 0.2 \times 0.2$ mm. the variation of Nusselt number is shown in the graph. Another aspect which we have considered in this study is the effect of thermal conductivity.

It is found that near the obstacle, heat transfer coefficient increases, which indicates that the presence of obstacle enhances the heat transfer coefficient and Nusselt number. The shape of heat transfer curves near the obstacle is shown in the enlarge view of graph.

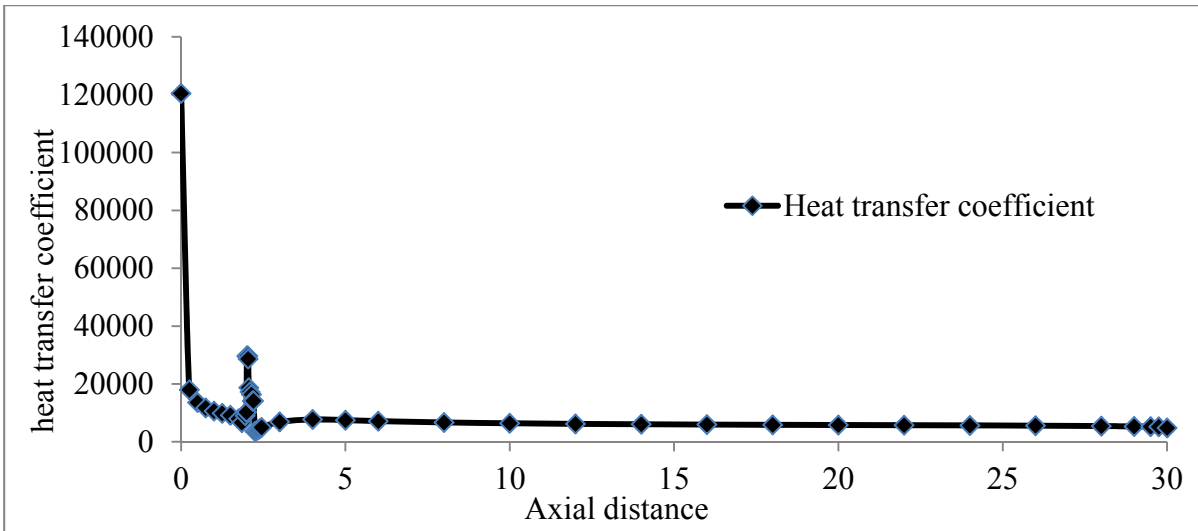


Figure 8: Variation of heat transfer coefficient along the length of microchannel

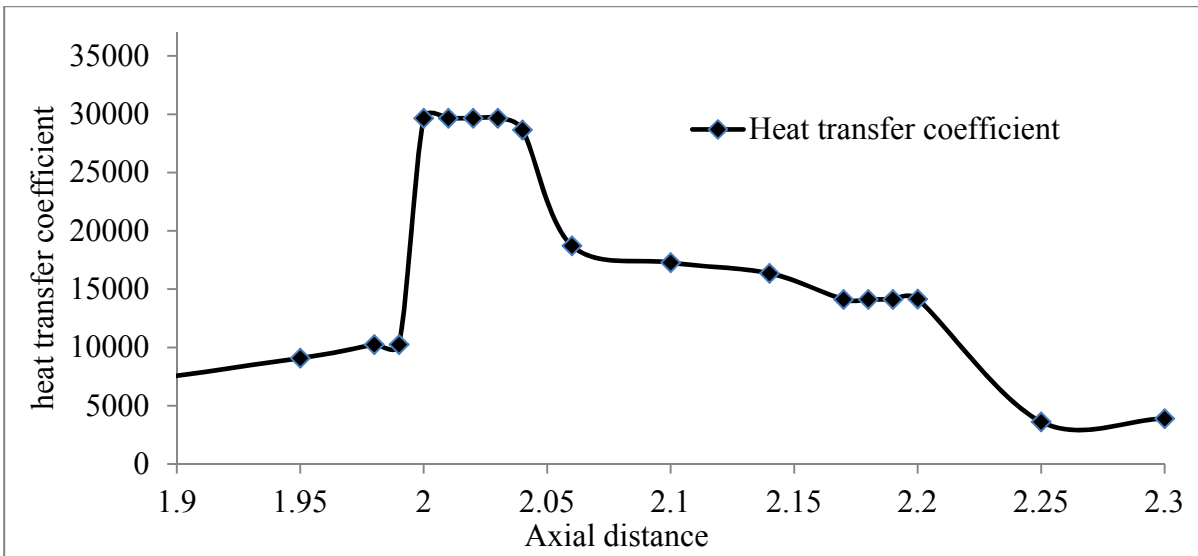


Figure 9: Enlarge view of heat transfer coefficient

The variation of Nusselt number along the length of the channel is plotted on the graph for different material. Nusselt number follows the shape of the obstacle roughly. Five different materials have been used for the analysis. Their conductivity varies from 7.86 to 429. Thermal conductivity is lowest for bismuth and highest for silver. In between them constantan, bronze and aluminium are present.

From the graph it has been found that the rise in Nusselt number depends on the thermal conductivities of the material respectively. Highest variation in Nusselt number is found in silver followed by aluminium, bronze, constantan and last bismuth.

Numerical Simulations were carried out considering following effects:

- A. Effect of thermal conductivity on the heat transfer
- B. Effect of position of obstacle
- C. Effect of shape of obstacle
- D. Use of model (laminar and turbulent)

A. Effect of thermal conductivity on heat transfer:

A(i). Effect of thermal conductivity when obstacle is placed at 2 mm from inlet:

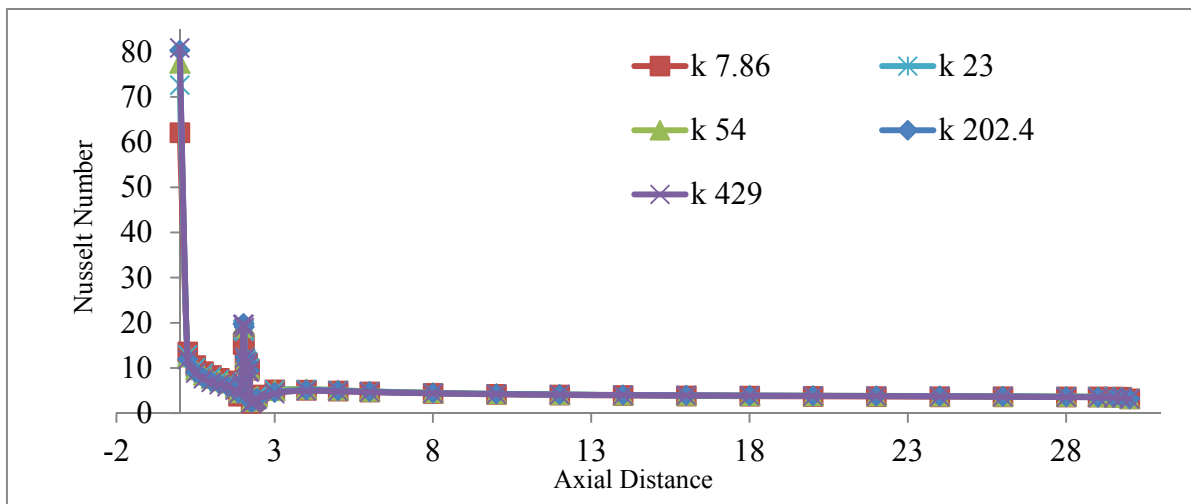


Figure 10 : Effect of thermal conductivity on Nusselt number when obstacle is at 2 mm from inlet

As the thermal conductivity increases, there is an increase in the height of curve in the obstacle region. Higher Nusselt number is found in silver which has the highest thermal conductivity among them. While bismuth show low Nusselt curve as its thermal conductivity is low.

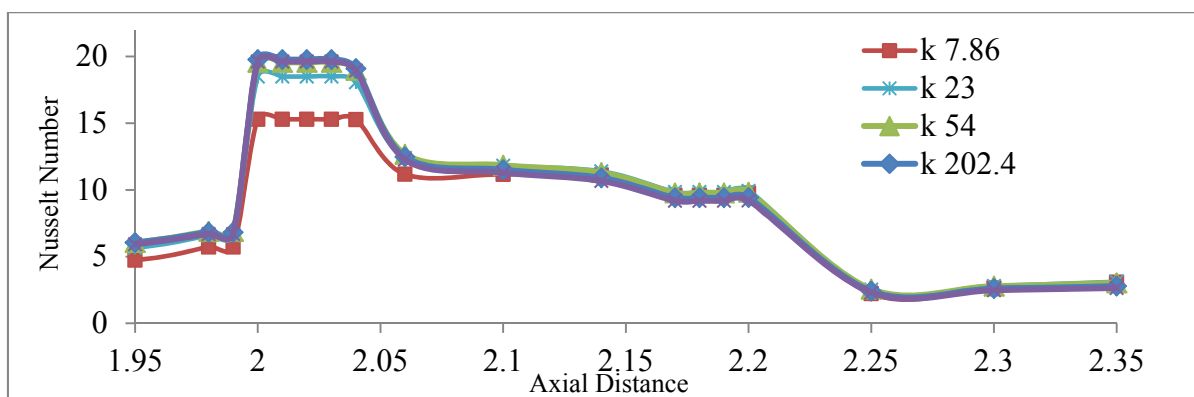


Figure 11: Enlarge view of variation of Nusselt number due to thermal conductivity when obstacle is at 2 mm from inlet

In enlarge view of Nusselt Number the shape of Nusselt curve can be seen. Nusselt curve climb at the front face of obstacle and falls down on the rear side obstacle.

A(ii). Effect of thermal conductivity when two obstacle at 2 mm and 20 mm from inlet:

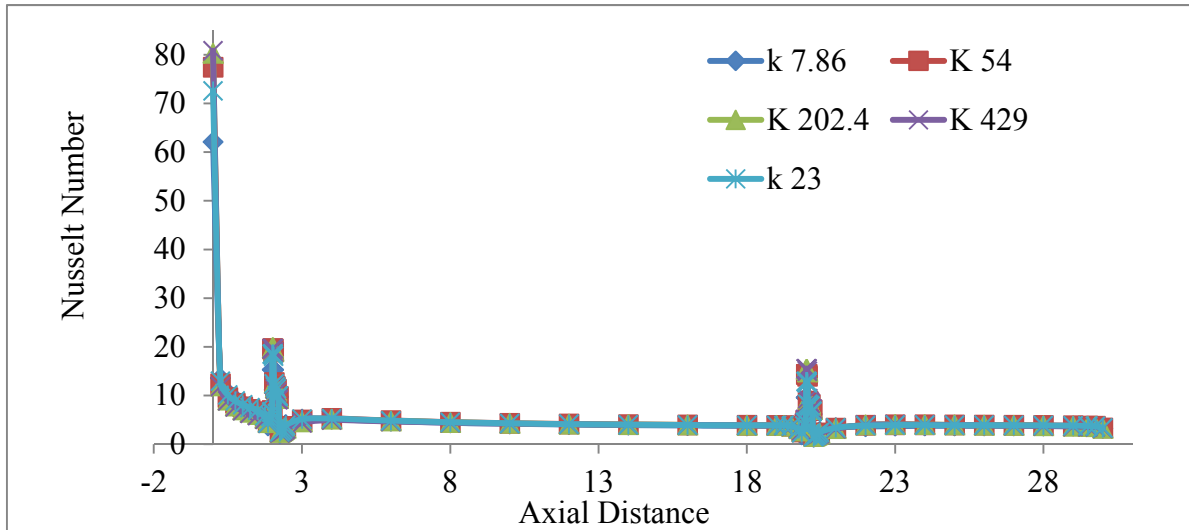


Figure 12: Effect of thermal conductivity on Nusselt Number

In another set of simulation, the same effect is seen, which supports the theory of higher thermal conductivity relation with Nusselt number. In this case, two obstacle is placed at 2 mm and 20 mm, variation near the obstacle zone is plotted below. In this case, silver with thermal conductivity with 429 has higher curve in obstacle region.

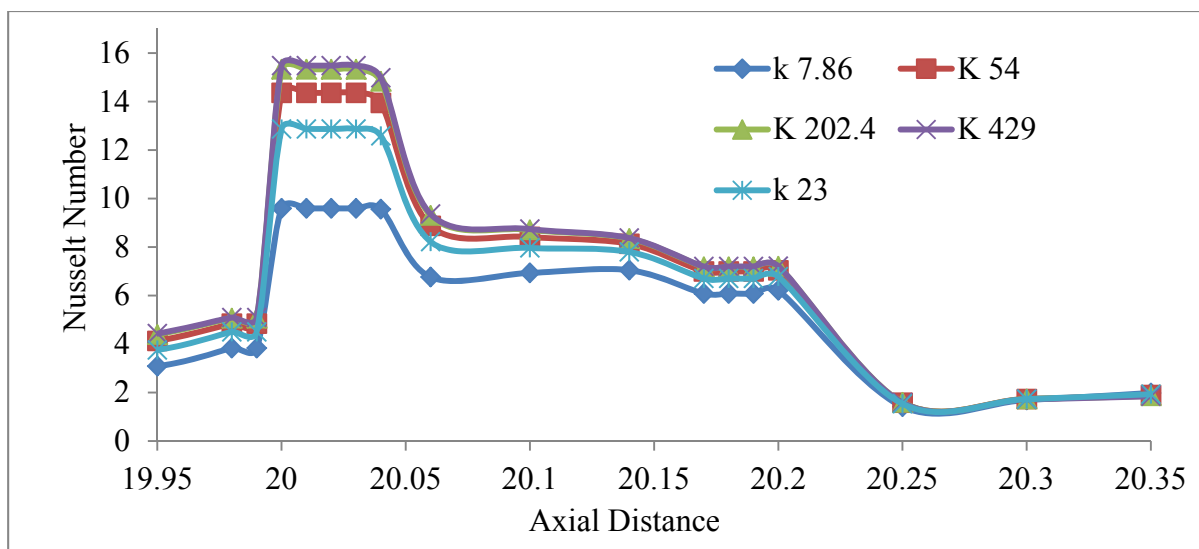


Figure 13: Enlarge view of variation of Nusselt Number due to thermal conductivity when obstacle is 20 mm from inlet

From the enlarge view of Nusselt Number graph, it can be seen that higher thermal conductivity of material leads to higher local Nusselt number near obstacle.

A(iii). **Effect of thermal conductivity when obstacle at 2 mm from inlet and k-ε model were used:**

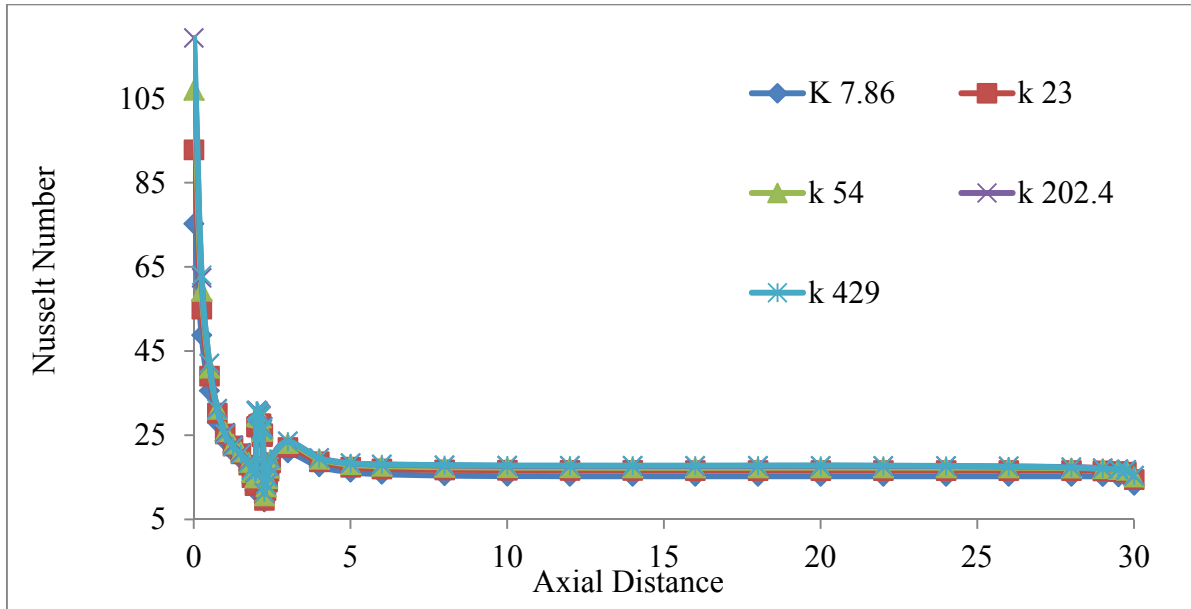


Figure 14: Effect of thermal conductivity on Nusselt number using k-ε model when obstacle at 2 mm from inlet

Above graphs also show that thermal conductivity effect on Nusselt number. From the graph, it can be interpreted that higher thermal conductivity leads to higher local Nusselt number near obstacle region.

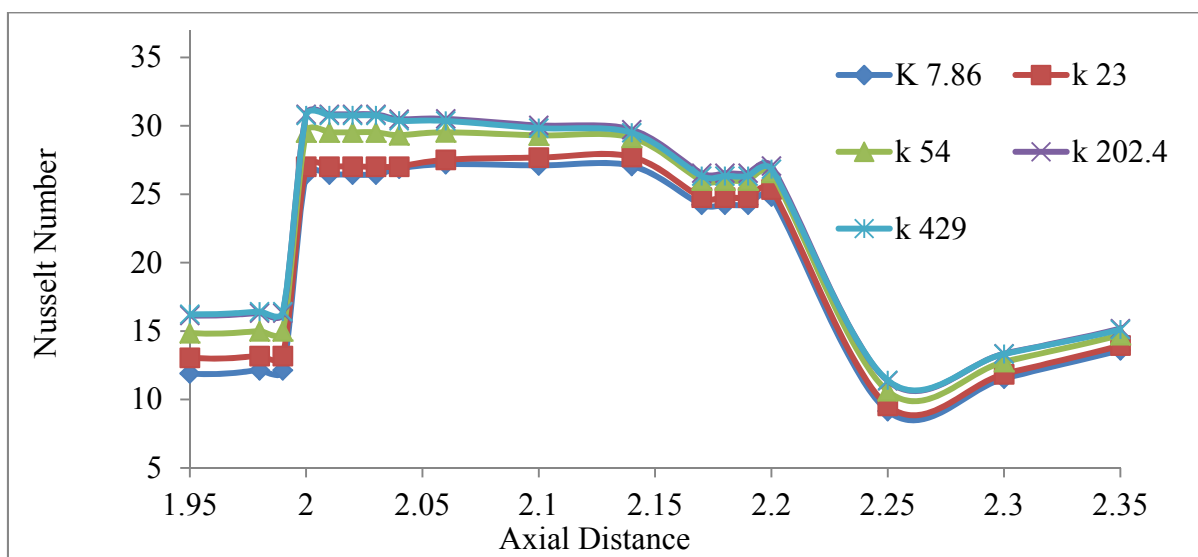


Figure 15: Enlarge view of variation of Nusselt number due to thermal conductivity

Enlarge view demonstrate the effect more clearly. Changing model from laminar to turbulent model does not effect the effect of thermal conductivity on Nusselt Number. But turbulent model account the eddy formation, due to which increase in Nusselt number is high in turbulent model compare to laminar model.

B. Effect of position of obstacle:

B(i). When obstacle is at 2 mm from inlet:

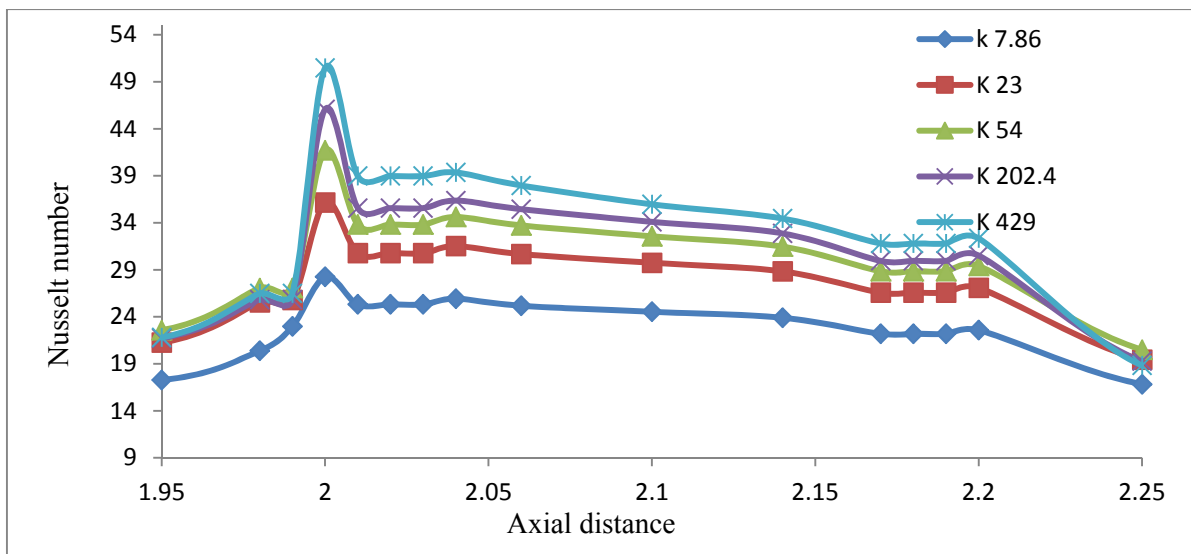


Figure 16: Variation of Nusselt number when position of obstacle is at 2 mm

It is noted from the graph plotted, that the position of obstacle in the flow field greatly effect the local Nusselt number. As the obstacle move away from the inlet, increase in the local Nusselt number decrease at the front face of obstacle. When comparing the graph of Nusselt number at 2 mm and 20 mm, it is found that rise in local Nusselt number when the obstacle is near to inlet region.

B(ii). When obstacle is at 20 mm from inlet:

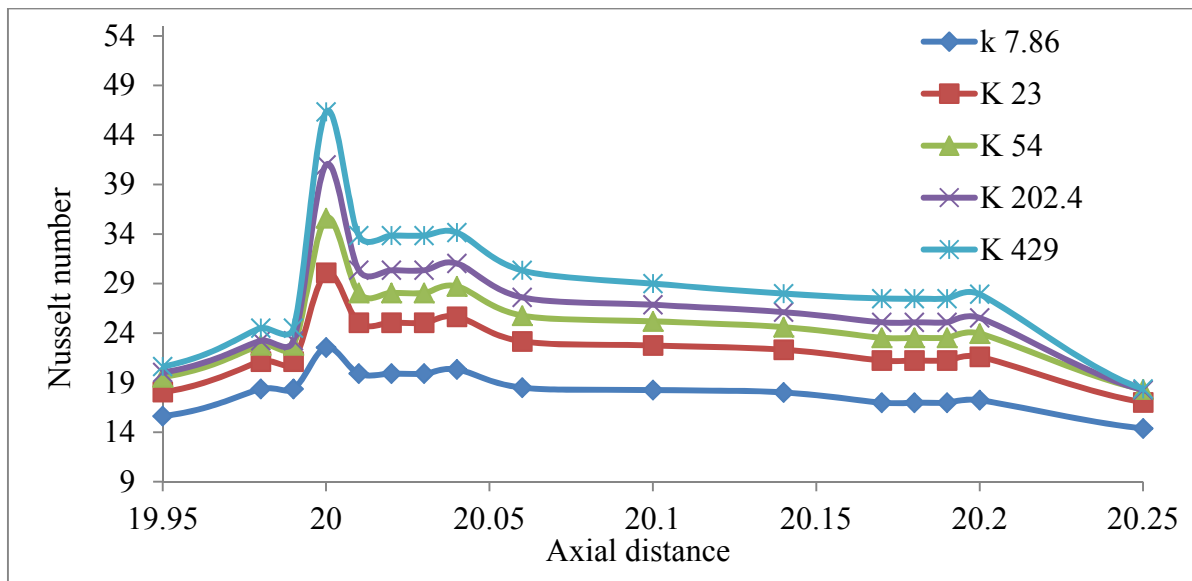


Figure 17 : Variation of Nusselt number when position of obstacle is at 20 mm

C. Effect of shape of obstacle:

In the study, two different shape of obstacle were used. Set of numerical simulation were done on both, and brought some results

C(i). Full rectangular obstacle:

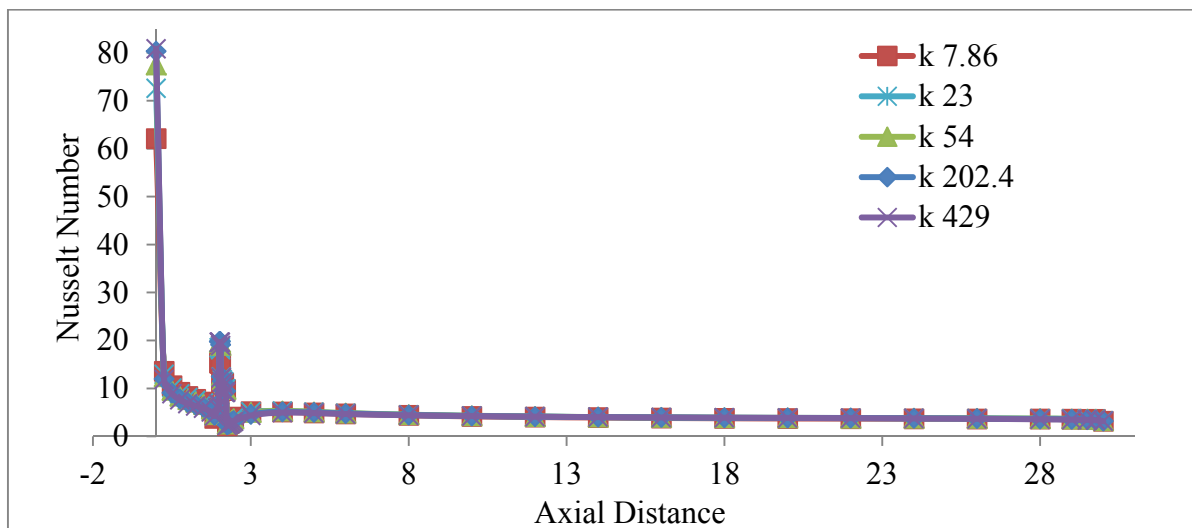


Figure 18: Variation of Nusselt number when full obstacle is placed in the flow field considering Laminar flow

A full rectangular obstacle is placed at 2 mm from inlet and variation of Nusselt Number is plotted on graph. In the enlarge view shape of Nusselt curve can be examined.

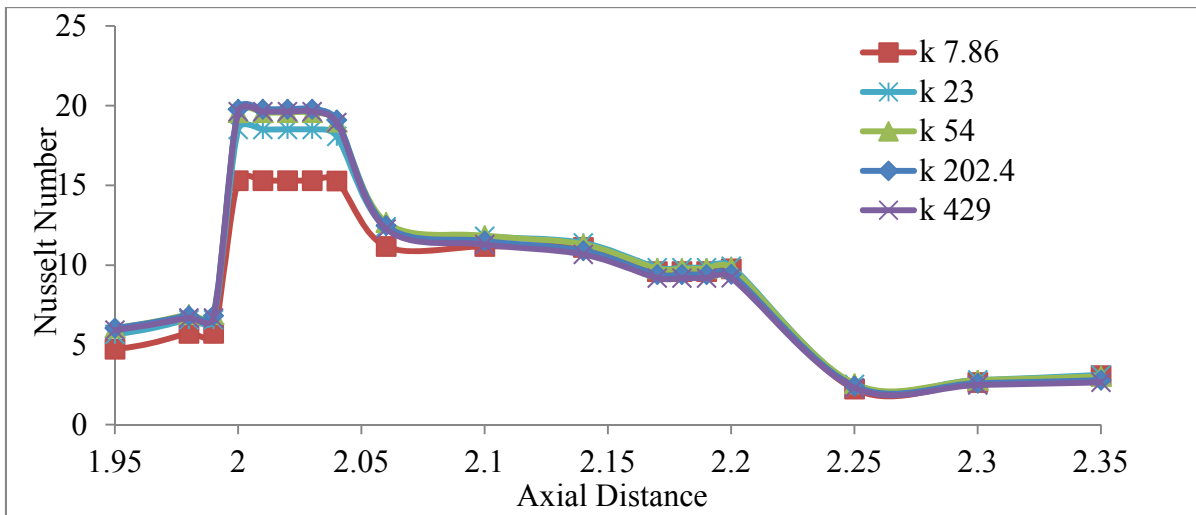


Figure19: Enlarge view of Nusselt number curve near the obstacle region

Enlarge view of Nusselt number show the variation of Nusselt number near obstacle region. At front face of obstacle Nusselt number increases sharply, and disturbance created by obstacle remains in flow field along the microchannel length. In this case shape of obstacle is full length normal to the stream lines. Obstacle disturbs streamlines and degree of disturbance is high at the front face of obstacle due to which a sharp rise in Nusselt number is found at front face.

In another set of simulation, variation of Nusselt Number for full obstacle using k-ε model is plotted on the graph. In this case, local Nusselt number increases sharply as compared to laminar flow. The graph shows the nature of Nusselt number when considering the turbulent flow across the channel.

C(ii). Full obstacle considering turbulent flow:

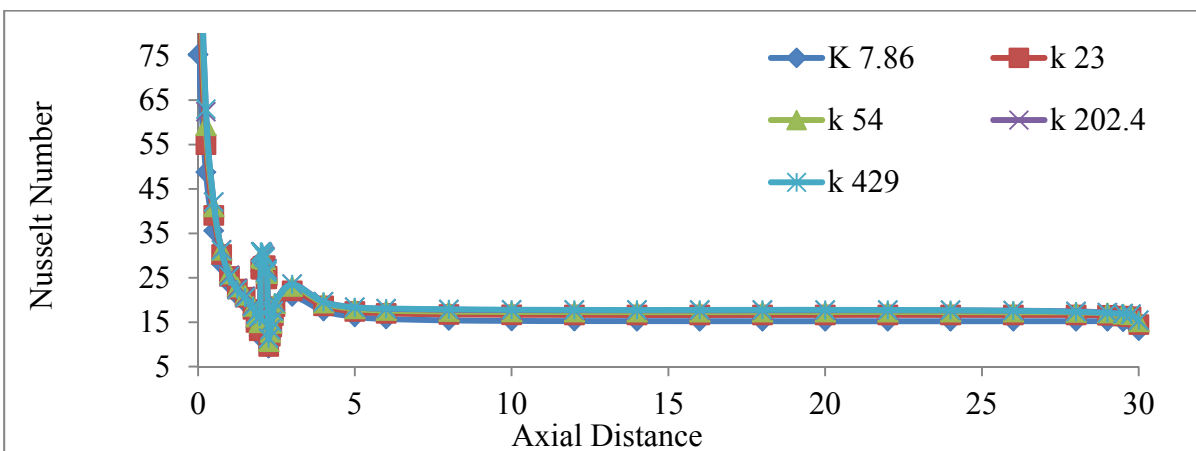


Figure 20: Variation of Nusselt number when full obstacle is placed in the flow field considering turbulent flow

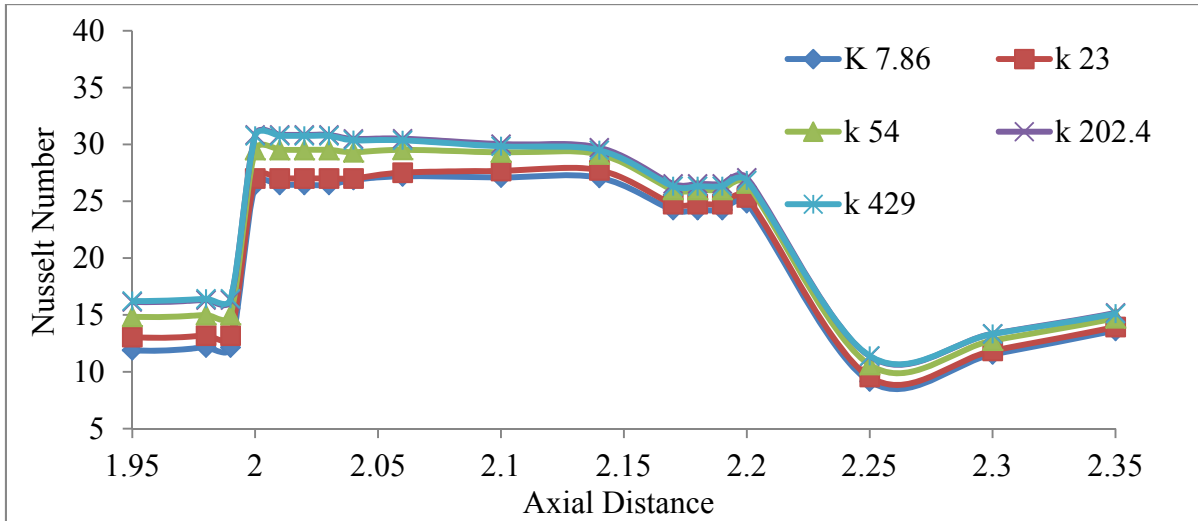


Figure 21: Enlarge view of Nusselt number curve near obstacle region

In the graph below, shows the variation of Nusselt Number for full and half obstacle for silver with thermal conductivity 429 using laminar model. From the graph, it can be concluded easily that local Nusselt number for the half obstacle is higher than full obstacle. From this set of simulation, it can also be concluded that half obstacle provide better mixing in between the fluid layers, which enhance heat transfer.

C(iii). Comparison of full obstacle and half obstacle:

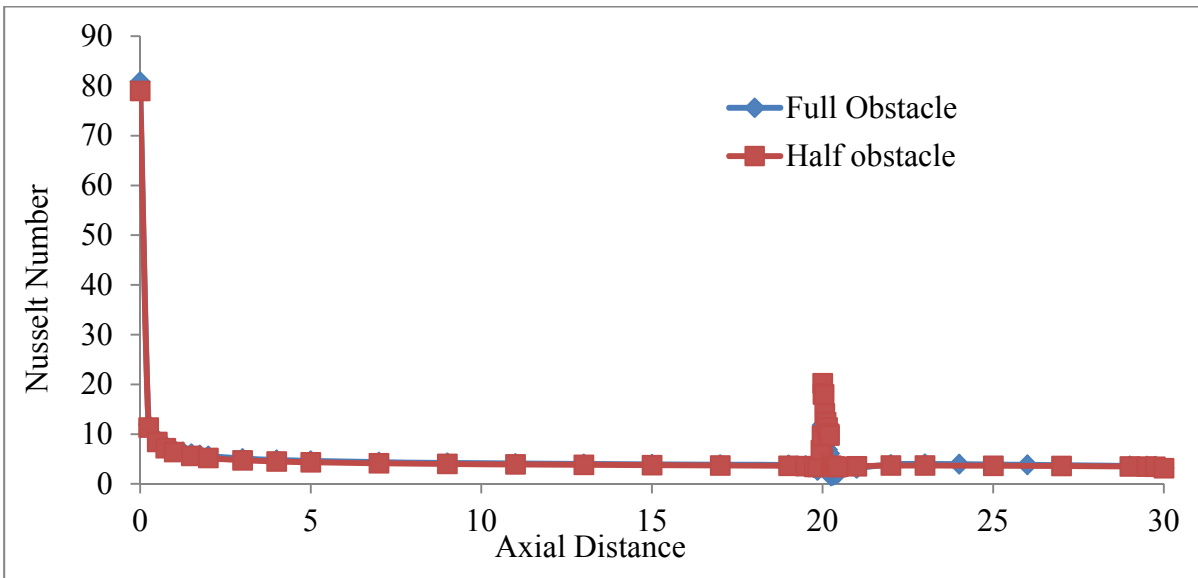


Figure 22: Comparison of Nusselt number for full and half obstacle

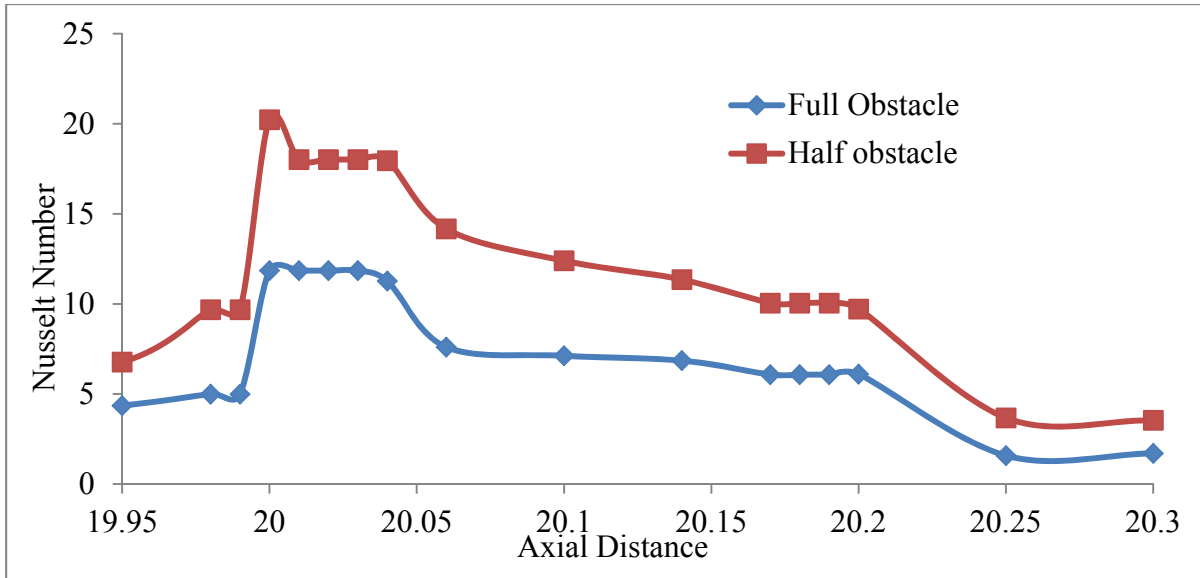


Figure 23: Enlarge view of Nusselt number for full and half obstacle

As the enlarge view of Nusselt curve concludes that higher local Nusselt number is obtained in half obstacle. The reason behind this variation is that in full obstacle fluid pass over the surface while in half obstacle, surface of obstacle divides the fluid flow in two streams, which leads to higher surface area of obstacle comes directly contact to fluid and at rear face of obstacle both streams of initial divided fluid mixes again and enhances the heat transfer.

Half obstacle:

In the second case, another model was used. A half obstacle were used and placed on the centre of channel bottom wall. After a set of simulations following result are obtained. Variation of Nusselt number is plotted on graph. In this case, flow is considering as laminar though presence of obstacle. Variations of all materials are plotted.

C(iv). Half obstacle considering laminar flow.

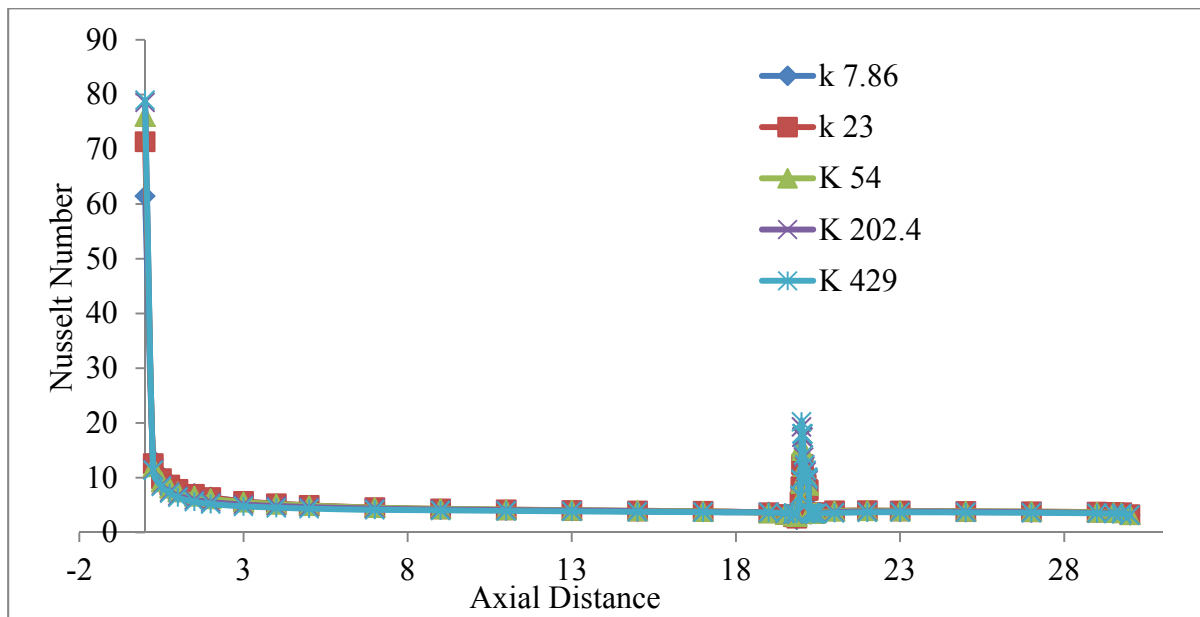


Figure 24: Variation of Nusselt number when half obstacle is placed in the flow field considering laminar flow

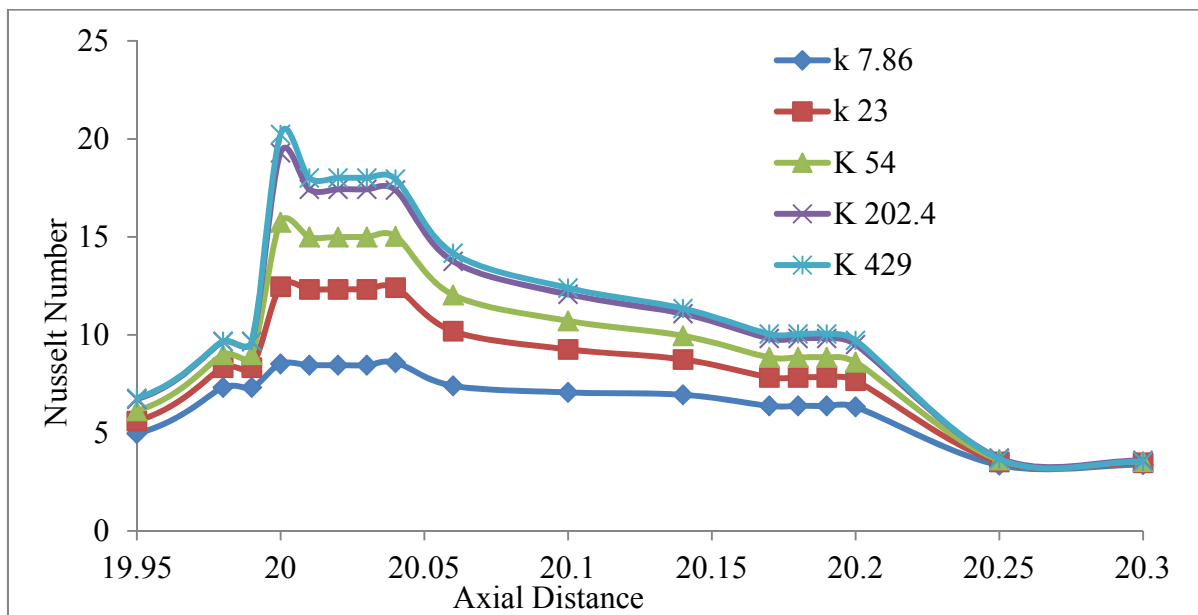


Figure 25: Enlarge view of Nusselt number curve near the obstacle region

In another set of simulation, half obstacle model is simulated in turbulent model, their corresponding graph are plotted on graphs. The height of Nusselt curves varies with the thermal conductivities respectively. But the local Nusselt number increase with the use of turbulent model.

In this case turbulent model is essential as the fluid divides in two streams due to presence of half obstacle which tend to form eddies at the rear face of obstacle. As turbulent model takes account of eddies formation.

C(v). Half obstacle considering turbulent flow:

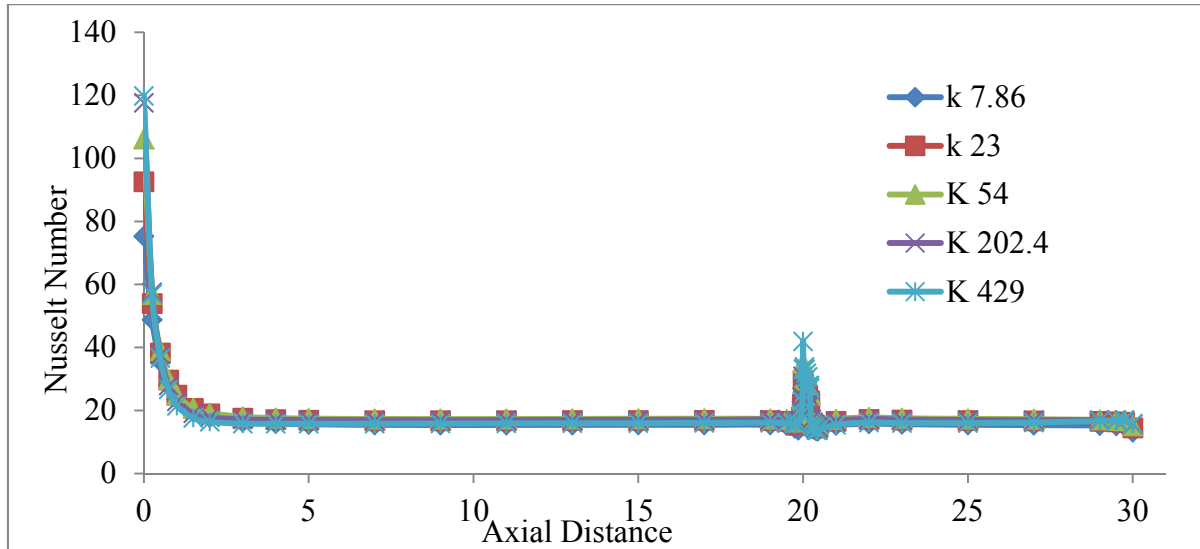


Figure 26: Variation of Nusselt number when half obstacle is placed in the flow field considering turbulent flow

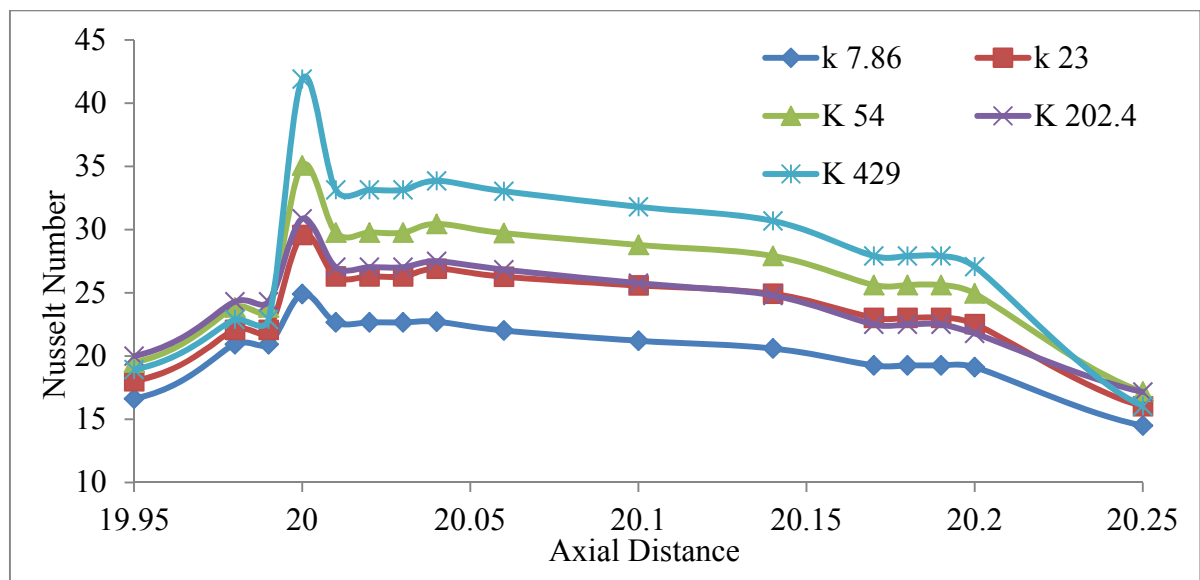


Figure 27: Enlarge view of Nusselt number curve near the obstacle region using turbulent model

Again from another set of simulation, it is found that half obstacle provides the higher local Nusselt number compared to full obstacle. Graph has been plotted for silver material which

has the highest thermal conductivity among other materials. In this case turbulent model is used. It can be concluded from the results that model does not have any effect when different shapes obstacle are used.

C(vi). Comparison of full and half obstacle using turbulent model:

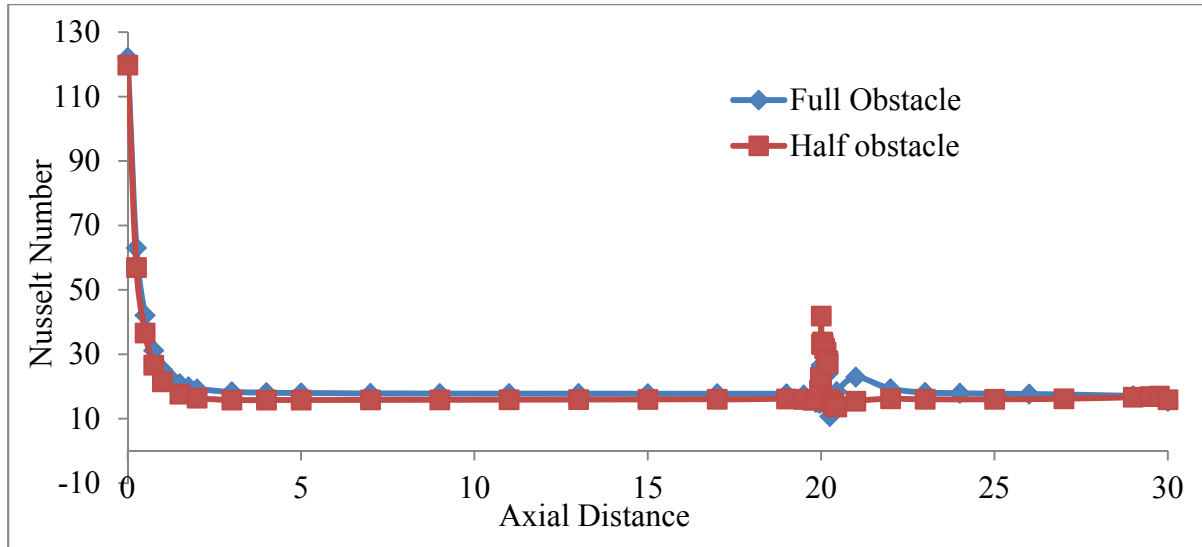


Figure 28: Comparison of Nusselt number for full and half obstacle using turbulent model

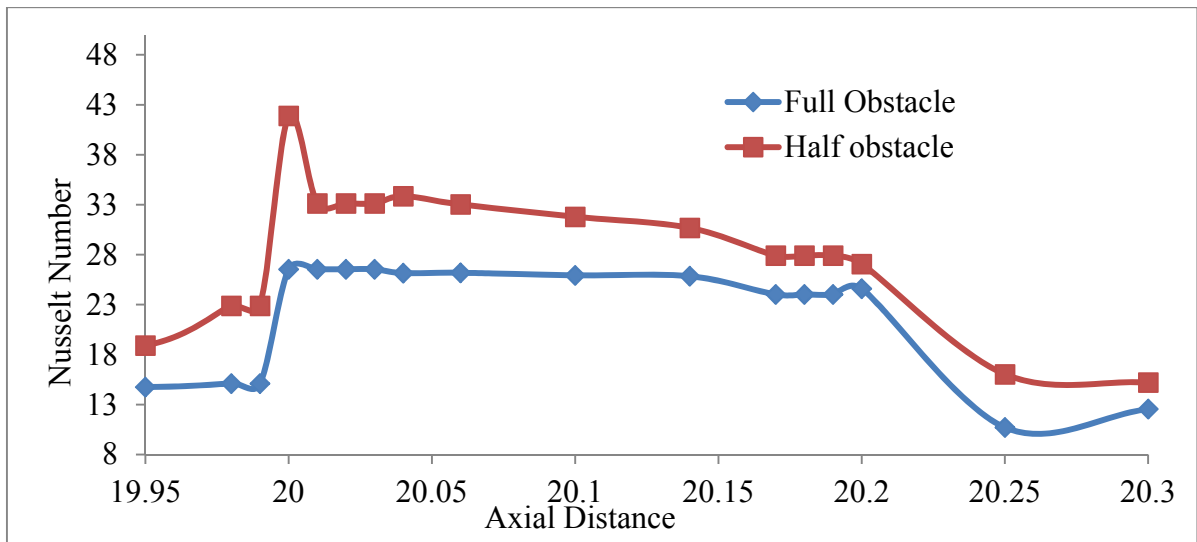


Figure 29: Enlarge view of Nusselt number for full and half obstacle using turbulent model

D. Effect of laminar/turbulent model:

In this section of results, laminar and turbulent model were examined, and their effect on the heat transfer. As in turbulent model two new parameters and their corresponding equation are involved, turbulent model can be easily acquired for eddy flow. These two parameters are

turbulent kinetic energy (k) and dissipation rate (ϵ) which independently modelled two new governing equations along with the other three conservation equations.

A set of simulation were carried out to examine the effect of models on heat transfer. In these simulations silver is used and obstacle is placed at 20 mm for both full and half obstacle. The outcomes are presented below:

D(i). Difference of laminar and turbulent for full obstacle:

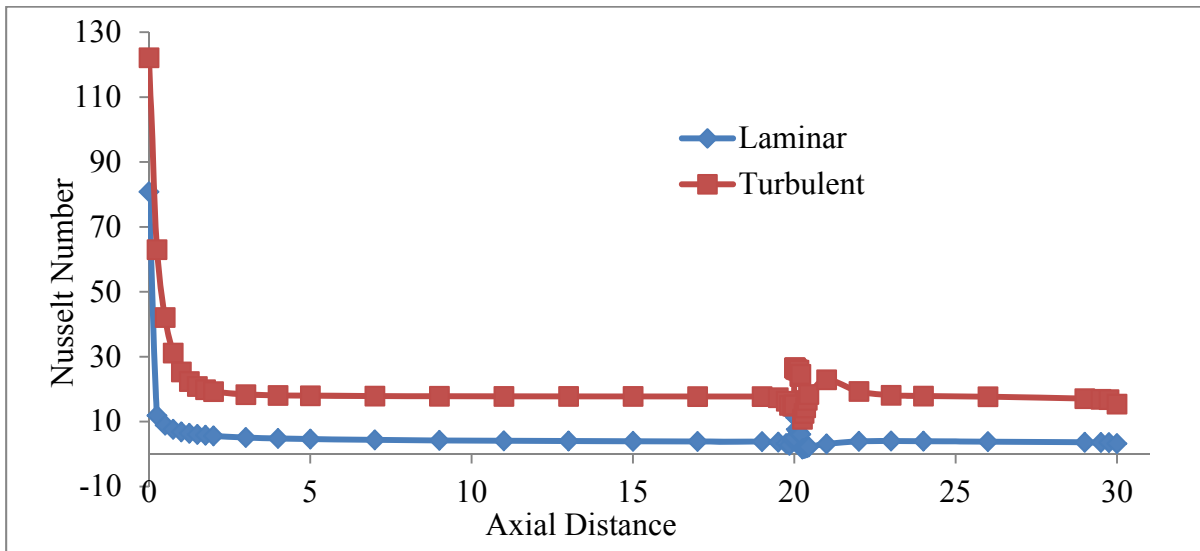


Figure 30: Variation of Nusselt number for full obstacle using laminar/turbulent model

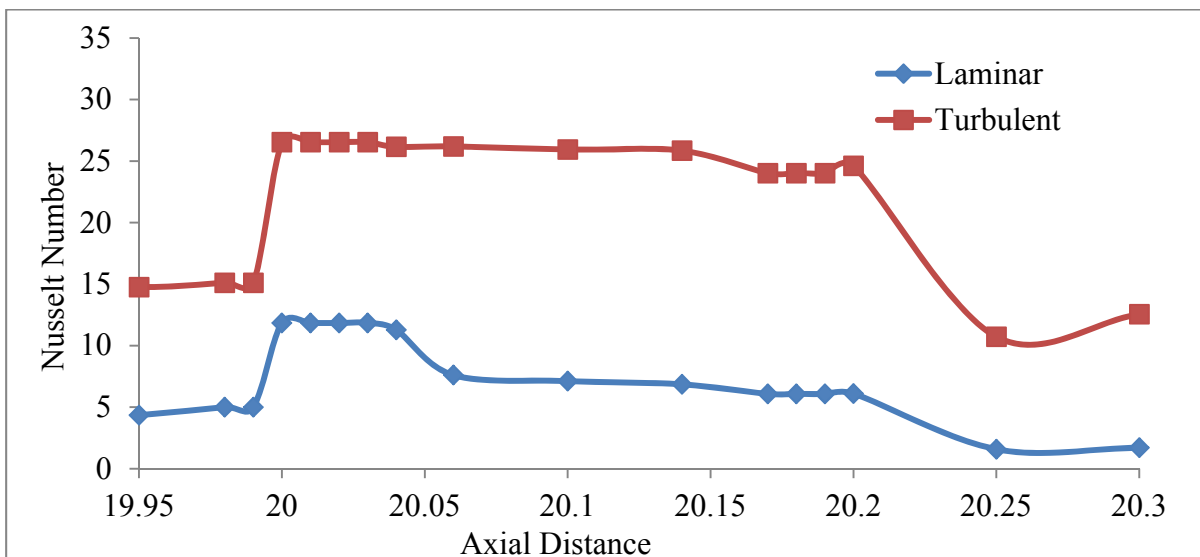


Figure 31: Enlarge view of Nusselt number for full obstacle near the obstacle zone.

It can be concluded from the graph, that higher local Nusselt number is found in turbulent model for full obstacle.

D(ii). Difference of laminar and turbulent for half obstacle:

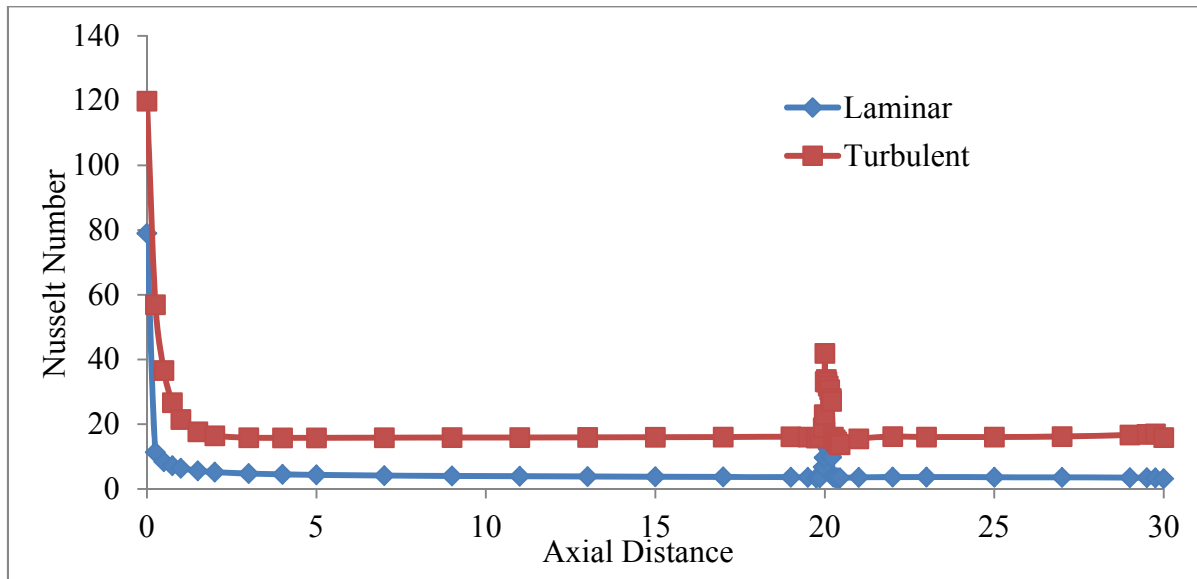


Figure 32: Variation of Nusselt number for half obstacle using laminar/turbulent model

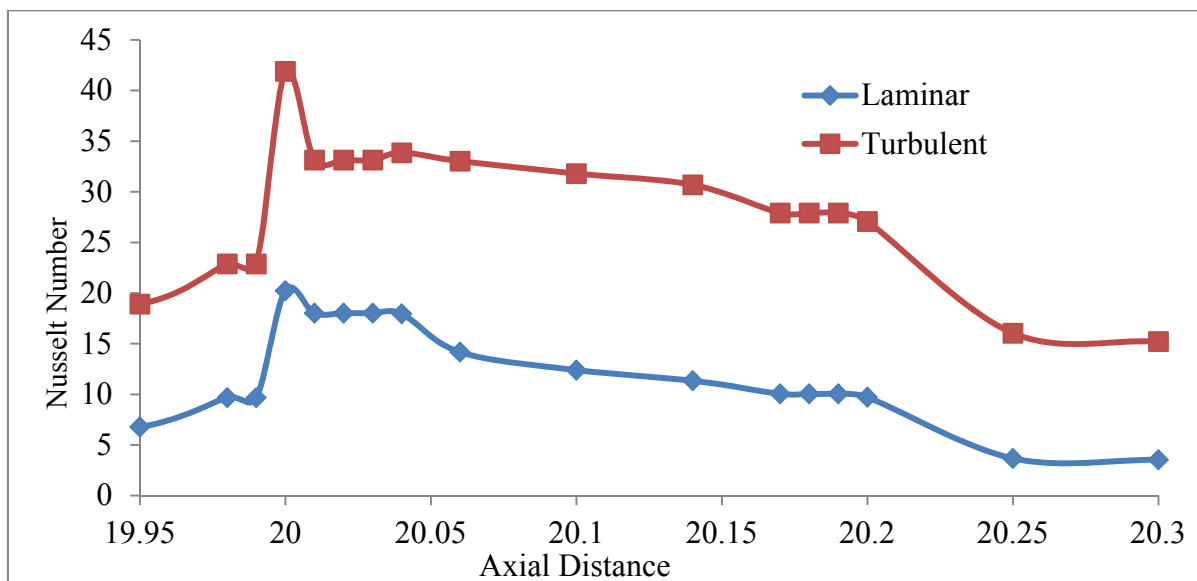


Figure 33: Enlarge view of Nusselt number near the obstacle zone.

Again in this case also, turbulent model shows higher local Nusselt number near the obstacle zone. It does not the account of change of shape of obstacle. It independently calculates the Nusselt number from other factors.

CONCLUSION

In this work three dimensional numerical investigation microchannel with obstacle placed at different positions. The simulation performed takes the following effect in to account (a) thermal conductivity, (b) position of obstacle in the channel, (c) shape of obstacle and (d) model used in simulation.

From the simulation performed following conclusion are made:

1. Thermal conductivity of the solid to fluid ratio is the one of the important factor which enhances the heat transfer coefficient. From the graph plotted, shows clearly, that material thermal conductivity directly correlated to Nusselt number variation. Higher thermal conductivity of the substrate leads to higher Nusselt number. From the list of materials given in Table no.1 silver has the highest thermal conductivity, hence in each case, average Nusselt number is highest for silver.
2. The second important parameter found in the analysis is the position of obstacle. Position of obstacle in the flow field varies the local Nusselt number along the length. When the obstacle is place at 2 mm from the inlet in developed zone, local Nusselt number increase high and the effect of disturbance created by obstacle is seen along the length.
3. Shape of obstacle is also important parameter found in the analysis. Shape of obstacle disturb the flow and create turbulence/eddies. In case of full obstacle is found that the increase in Nusselt number is not high as compared to half obstacle. Half obstacle creates high disturbance in the flow, which increases mixing between the different fluid layers.
4. Use of laminar model or turbulent model is dependent on the Reynolds number. Though the Reynolds number is low but due to presence of obstacle eddies formed at rear face of obstacle. Therefore it is necessary to simulate the cases in both models. And it is found that higher Nusselt number is found in turbulent flow model for both half and full obstacle. Laminar model under predicts the Nu value compared to turbulent model.
5. Another important effect found in this analysis is the temperature difference between wall and fluid near the obstacle region. Along the length of obstacle temperature difference increases but in the obstacle region this difference decreases.

REFERENCES

1. Khandekar S., Moharana M. K., 2014, Some applications of micromachining in thermal-Fluid engineering, Chapter in: Introduction to Micromachining, 2nd Edition, Editor: Dr. V. K. Jain, Narosa Publishing House.
2. Tuckerman D.B., Pease R.F.W., 1981, High-performance heat sinking for VLSI, IEEE Electron Device Letters, 2(5), pp. 126–129.
3. Muralidhar K. and Biswas G., 2006, Advanced Engineering Fluid Mechanics, Narosa Publication House, New Delhi, India.
4. Cengel, Y.A., Heat Transfer: A Practical Approach, McGraw-Hill, New York, USA 2003.
5. Tullius J.F., Tullius T.K., Bayazitoglu Y., 2012 , Optimization of short micro pin fins in minichannels, International Journal of Heat and Mass Transfer 55, pp. 3921–3932
6. Wang Y., Houshmand F., Elcock D., Peles Y., 2013, Convective heat transfer and mixing enhancement in a microchannel with a pillar, International Journal of Heat and Mass Transfer 62, pp. 553–561
7. Peles Y., Ali K., Mishra C., Kuo C.J., Schneider B., 2005, Forced convective heat transfer across a pin fin micro heat sink, International Journal of Heat and Mass Transfer 48, pp. 3615–3627
8. Liu M., Liu D., Xu S., Chen Y., 2011, Experimental study on liquid flow and heat transfer in micro square pin fin heat sink, International Journal of Heat and Mass Transfer 54, pp. 5602–5611
9. Ndao S., Lee H.J., Peles Y., Jensen M.K., 2012, Heat transfer enhancement from micro pin fins subjected to an impinging jet, International Journal of Heat and Mass Transfer 55, pp. 413–421
10. Khan W.A., Culham J.R., and Yovanovich M.M., 2008, Modeling of cylindrical pin-fin heat sinks for electronic packaging, IEEE transactions on Components and Packaging Technology, 31(3) pp. 536-545
11. Roth R., Lenk G., Cobry K., Woias P., 2013, Heat transfer in freestanding microchannels with in-line and staggered pin fin structures with clearance, International Journal of Heat and Mass Transfer 67, pp. 1–15
12. Qu W., Ho A.S., 2008, Liquid single-phase flow in an array of micro-pin-fins—part I:Heat transfer characteristics, Journal of Heat Transfer, 130(12) / 122402 pp. 1-11

13. Qu W., Ho A.S., 2008, Liquid single-phase flow in an array of micro-pin-fins—part II: Pressure drop characteristics, *Journal of Heat Transfer*, 130/ 124501 pp.1-4
14. Dutta S, Panigrahi P. K., and Muralidhar K., 2008, Experimental investigation of flow past a square at an angle of incidence, *Journal of Engineering Mechanics*, 134 (9) pp. 788-803.
15. Mittal S., 2001, Computation of three-dimensional flows past circular cylinder of low aspect ratio, *Physics of Fluids*, 13(1) pp. 177–191
16. Seyf H.R., Layeghi M., 2010, Numerical analysis of convective heat transfer from an elliptic pin fin heat sink with and without metal foam insert, *Journal of Heat Transfer*, 132 / 071401 pp. 1-9
17. Jasperson B.A., Jeon Y., Turner K.T., Pfefferkorn F.E., and Qu W., 2010, Comparison of micro-pin-fin and microchannel heat sinks considering thermal-hydraulic performance and manufacturability, *IEEE transactions on Components and Packaging Technology*, 33 (1) pp. 148-160
18. Qu W., Mudawar I., 2002, Analysis of three-dimensional heat transfer in microchannel heat sinks, *International Journal of Heat and Mass Transfer*, 45, pp. 3973–3985
19. Qu W., Mudawar I., 2002, Experimental and numerical study of pressure drop and heat transfer in a single-phase microchannel heat sink, *International Journal of Heat and Mass Transfer*, 45, pp. 2549–2565
20. Abel M. Siu-Ho, Qu W., Pfefferkorn F.E., 2007, Experimental study of pressure drop and heat transfer in a single-phase micropin-fin heat sink, *Journal of Electronic Packaging*, Vol. 129 (4), pp. 479-487
21. Zhou M., Dong X.G., Lei C., Jian LI., LiJun Z., 2012, Analysis of flow and heat transfer characteristics of micro-pin fin heat sink using silver nano-fluids, *Sci China Tech Sci*, 55(1), pp. 155-162
22. Guo Z.Y., Li Z.X., 2003, Size effect on micro-scale single-phase flow and heat transfer, *International Journal of Heat and Mass Transfer*, 46, pp. 149-159.
23. Lee P.S., Garimella S.V., Liu D., 2005, Investigation of heat transfer in rectangular microchannels, *International Journal of Heat and Mass Transfer* 48, pp 1688–1704
24. Hetsroni G., Mosyak A., Pogrebnyak E., Yarin L.P., 2005, Fluid flow in microchannels, *International Journal of Heat and Mass Transfer*, 48, 1982–1998
25. Morini G.L., 2005, Viscous heating in liquid flows in microchannels, *International Journal of Heat and Mass Transfer* 48, pp. 3637–3647

26. Hetsroni G., Mosyak A., Pogrebnyak E., Yarin L.P., 2005, Heat transfer in microchannels: Comparison of experiments with theory and numerical results, *International Journal of Heat and Mass Transfer* 48, pp. 5580–5601
27. Lee P.S., Garimella S.V., 2006, Thermally developing flow and heat transfer in rectangular microchannels of different aspect ratios. *International Journal of Heat and Mass Transfer* 49, pp. 3060–3067
28. Moharana M.K., Singh P.K., Khandekar S., 2012, Optimum Nusselt number for simultaneously developing internal flow under conjugate conditions in a square microchannel, *Journal of Heat Transfer*, 134 / 071703 pp.1–10
29. Moharana M.K., Agarwal G., Khandekar S., 2011, Axial conduction in single-phase simultaneously developing flow in a rectangular mini-channel array, *International Journal of Thermal Sciences*, 50(6) 1001-1012.
30. Moharana M.K., Khandekar S., Numerical study of axial back conduction in microtubes, 39th National Conference on Fluid Mechanics and Fluid Power (FMFP2012), 13-15 December 2012, Surat, India.
31. Moharana M.K., Khandekar S., 2013, Effect of aspect ratio of rectangular microchannels on the axial back-conduction in its solid substrate, *International Journal of Microscale and Nanoscale Thermal and Fluid Transport Phenomena*, 4(3-4) 1-19.
32. Kumar M., Moharana M.K., Axial wall conduction in partially heated microtube, 22nd National and 11th International ISHMT-ASME Heat and Mass Transfer Conference, 28-31 December 2013, Kharagpur, India.
33. Tiwari N., Moharana M.K., Sarangi S.K., Axial wall conduction in partially heated microtube, 40th National Conference on Fluid Mechanics and Fluid Power (FMFP2012), 12-14 December 2013, Hamirpur, India.